Successive Approximation Coding for Distributed Matrix Multiplication

Shahrzad Kiani, *Graduate Student Member, IEEE,* and Stark C. Draper, *Senior Member, IEEE*

Abstract—**Coded distributed computing was recently introduced to mitigate the effect of stragglers on distributed computing. This paper combines ideas of approximate computing with coded computing to further accelerate computation. We propose *successive approximation coding* (SAC) techniques that realize a tradeoff between accuracy and speed, allowing the distributed computing system to produce approximations that increase in accuracy over time. If a sufficient number of compute nodes finish their tasks, SAC exactly recovers the desired computation. We theoretically provide design guidelines for our SAC techniques, and numerically show that SAC achieves a better accuracy-speed tradeoff in comparison with previous methods.**

Index Terms—**Successive approximation, approximated computing, coded computing, stragglers**

I. INTRODUCTION

Distributed computing is necessary for handling modern real-time data analytics and computationally intensive applications such as genome and DNA sequencing, and deep learning. To meet this need, distributed systems are increasing in complexity and size. This gives rise to novel challenges that plague today's distributed computing systems. These include failures, stragglers, communication bottlenecks, and security and privacy issues. The emerging field of coded distributed computing (CDC) comprises a set of promising techniques that deal with these challenges [1]–[11]. CDC employs ideas from coding theory to form redundant computations such that only some sufficient number of computing nodes (called workers) need to complete their tasks before desired computation can be recovered. The number of required workers is called the *recovery threshold*. In distributed computing systems that consist of tens or hundreds of workers (or even more for emerging Federated learning applications), recovery thresholds need to be large because of the tradeoff between recovery threshold and per-worker communication load. In large-scale systems, typical CDC strategies minimize expensive communication from each worker by increasing the recovery threshold. However, the larger recovery threshold is, the lower tolerance the system has for failures, stragglers, attackers, or colluding nodes. Lower tolerance can result in unnecessary delay, power consumption, and the waste of underlying hardware resources (such as CPUs and GPUs). That said, the fundamental limits

on recovery threshold and per-worker communication load can be improved by relaxing requirements for exact recovery.

In this paper, we combine ideas from approximate computing with CDC, producing a sequence of approximations of our target computation that are increasingly accurate. In analogy with the recovery threshold, we introduce a new metric *approximate threshold* that quantifies the number of workers required for approximate recovery within some degree of error. We identify a tradeoff between the approximate threshold and the magnitude of the error and provide explicit CDC methods that illustrate this tradeoff. Our approximate CDC methods hold promise for many modern error-tolerant applications such as learning deep neural network models. In these applications, approximated results are acceptable and often inevitable. In the remainder of this introductory section, we first overview prior CDC schemes to provide the proper context to present our contributions. We then detail our contributions and outline the remainder of the paper.

A. Background

1) Polynomial-based CDC: The foundation of CDC schemes is built on novel methods for the distributed multiplication of a pair of matrices A and B to form their product AB. Probably the largest group of CDC schemes designed for distributed matrix multiplication are based on polynomials. In all, a pair of *encoding* polynomials are used separately to encode the A and B matrices. Computing the product of these encoding polynomials results in another polynomial, called the *decoding* polynomial. The degree of the decoding polynomial equals the sum of the degrees of the encoding polynomials. Each worker is tasked with multiplying two encoding polynomials, both of which are evaluated at the same point. Each worker's evaluation point is distinct from other workers' evaluation points. The completion of a worker's task is equivalent to calculating the decoding polynomial at that worker's evaluation point. Once a sufficient number of workers complete their tasks, evaluations of the decoding polynomial are known at a sufficient number of points that polynomial interpolation can be applied and the decoding polynomial can be fully recovered. The desired matrix product AB is recovered from the interpolated decoding polynomial.

We group polynomial-based CDC schemes based on how they recover the AB product from the interpolated polynomial: *coefficient-based* or *point-based*. In the former group, the AB product is equal to one (or more) of the coefficients in the decoding polynomial. In the latter, a post-decoding calculation is required wherein the decoding polynomial is interpolated at

(new) points and the AB product is then recovered by linearly combining the new interpolated results. For example, Polynomial codes [4] are one of the earliest CDC constructions. They belong to the coefficient-based group because they recover the AB product by concatenating all the coefficients of the decoding polynomial. Another coefficient-based CDC scheme is MatDot codes [5]. The recovery threshold of Polynomial codes is reduced by MatDot codes, albeit at the cost of increased communication per worker. One of the coefficients in the decoding polynomial of MatDot codes is equal to the AB product. In [5], [9], [10], other coefficient-based CDC schemes are introduced that generalize and unify Polynomial and MatDot codes, providing a tradeoff between recovery threshold and per-worker communication load.

There are two features common to all these coefficient-based CDC constructions. The first is that both the encoding and decoding polynomials are expanded in the *monomial* basis, $1, x, x^2, \ldots$. The second is that the interpolation at the decoding phase requires the solution of a system of linear equations that involves a *Vandermonde* matrix with real-valued entries. Through Vandermonde-based interpolation, coefficient-based CDC schemes recover the AB product directly from the interpolated coefficients of the monomial basis. However, Vandermonde matrices defined over reals are ill-conditioning. The condition number of real Vandermonde matrices grows exponentially in the dimension of the matrix [12]. Ill-conditioning can lead to numerical problems when the inverse is taken to perform interpolation. In contrast, point-based CDC constructions are not limited to the monomial basis nor to Vandermonde-based interpolation. They can use better-conditioned bases but must extract the desired computation from their coefficients through post-decoding calculations. Despite the requirement of post-decoding calculations, the use of other (non-monomial) polynomial bases has benefits when compared to coefficient-based CDC constructions. For example, OrthoMatDot codes [13] use an *orthonormal* basis and *Chebyshev-Vandermonde* interpolation. This solves the ill-conditioning issue of MatDot codes. Another point-based CDC method is Lagrange coding [11] which uses the *Lagrange* polynomial basis. Using the Lagrange basis allows Lagrange codes to extend to more general multi-variate polynomial computing beyond matrix multiplication with guarantees of straggler resilience, security, and privacy. Lagrange codes use Vandermonde interpolation which can again lead to an ill-conditioned problem. In addition to MatDot codes, [13] applies a Chebyshev-Vandermonde decoder to Lagrange codes in order to mitigate ill-conditioning.

2) Approximation in CDC: While most CDC works to date limit themselves to exact recovery, some recent literature has combined approximation with earlier CDC schemes [14]–[20]. Motivated by [21], references [14] and [15] use different random-based sampling techniques first to compress A and B and then use MatDot codes to encode the data matrices. Due to the randomized compression of their input matrices, the recovery thresholds in both [14] and [15] are reduced. This accelerates recovery while providing only an approximation of the desired computation. In both [14] and [15], the compressing and coding steps are separate. Therefore, to provide another

estimate with lower error, the input matrices should be newly compressed and a new coding step need to be used for the new random samples of inputs. Another line of work [16] and [17] brings the idea of approximate computing to the encoding and decoding steps. Using maximum distance separable (MDS) codes, [16] and [17] guarantee accuracy improvement over time by intelligently prioritizing and allocating tasks among workers. These methods while effective, are applied only to matrix-vector multiplication. Their extension to matrix-matrix multiplication is non-trivial.

Approximation methods for matrix-matrix multiplication are introduced in [18] and [19] based on sketching. In [18] and [19] randomized pre-compression via sketching is used to reduce the dimension of input matrices, thereby, reducing the recovery threshold. In contrast to the aforementioned random sampling-based techniques ([14], [15]), references [18] and [19] jointly design the sketching step together with the coding step to minimize the recovery threshold while ensuring the required computation accuracy. Such optimal recovery threshold is achieved only in a probabilistic manner. In other words, there exists a non-zero probability of failing to recover the computation to the required accuracy. For us, the most relevant approximate CDC construction, and the one that motivated our work, is ϵ-*approximate* MatDot codes [20]. In [20], polynomial approximation techniques add a layer of approximation to MatDot codes. Through this approximation layer, the recovery threshold is roughly halved and the approximated computation is recovered with probability one. More details on [20] are provided in Sec. II-C.

B. Summary of Contributions

In this paper, we develop two novel approximate CDC methods. Each produces a sequence of increasingly accurate approximations of the desired calculation as more and more workers report in. We term this *successive approximation coding* (SAC) and call each approximation in the sequence a *resolution layer*. Our first method can be viewed as an extension of ϵ-approximate MatDot codes [20]. While [20] allows for a single resolution layer prior to exact recovery, our designs allow multiple resolutions. This enables the distributed system to stop sooner, whenever the resolution of the matrix product is satisfactorily high. In our first method, we divide resolution layers into groups. While resolution increases across layers, these increases are most significant across groups and comparatively negligible within the layers of a group. Our second method extends approximation recovery to point-based polynomial codes, such as OrthoMatDot codes [13] and Lagrange codes [11]. This method can be viewed as a limiting version of our first method where each group contains a single layer and accuracy improves every time an additional worker completes its task. We call our two methods "group-wise" and "layer-wise" SAC. Due to the grouping of the resolution layers in group-wise SAC, the approximate recovery improves in discrete steps (one step per group) as workers report in. For layer-wise SAC, the improvements are more continuous. We theoretically design our SAC methods in such a way that their error of approximation is minimized. Our simulation

results show that in comparison with ϵ-approximate MatDot codes [20], our methods require a lower number of workers for approximate recovery (i.e., a lower approximation threshold) to attain the same degree of error.

An outline for the rest of the paper is as follows. In Sec. II, we present the problem formulation that we consider. In Sec. III and IV, we introduce our two SAC methods in detail. In Sec. V, we experimentally show the benefits of each of our SAC methods. We conclude in Sec. VI.

II. PROBLEM FORMULATION

In this section, we first present the system model. We then discuss relevant performance measures. Finally, we detail previous CDC schemes that set the stage for our work.

A. System Model

We consider a distributed computing system that consists of a master and N workers. The job is to compute the matrix-matrix product AB, where $A \in \mathbb{R}^{N_x \times N_z}$ and $B \in \mathbb{R}^{N_z \times N_y}$. We partition A vertically into K equally-sized submatrices $A = [A_1, \ldots, A_K]$, where for any $k \in [K]$ that $N_z/K \in \mathbb{Z}$, A_k is a matrix of size $N_x \times N_z/K$[1]. Similarly, the B matrix is partitioned horizontally into K equally-sized submatrices $B^T = [B_1^T, \ldots, B_K^T]$, where B_k is a $N_z/K \times N_y$ matrix, $k \in [K]$. Due to this partitioning, the AB product can be calculated as a sum of K outer products, $AB = \sum_{k=1}^{K} A_k B_k$. We use the notation K to denote the *information dimension* of a code. The information dimension refers to the number of useful (non-redundant) computations into which the main computational job is partitioned. For a fair comparison, we fix both the information dimension, K, and the number of workers, N, across different CDC schemes in this paper.

B. Performance Metric

We use the following metrics throughout the paper to benchmark our proposed method against prior work.

Definition 1 (Recovery threshold): The recovery threshold is the number of workers required to complete their tasks for the master to be able to obtain the *exact* result. To denote the recovery threshold of a code, we use R_x with the subscript x indicating the type of the code. For example, for the codes that are used in this paper, their recovery thresholds are summarized in the second column of Table I. In CDC, $N - R$ can be thought of as the maximum number of stragglers that the distributed system can tolerate[2].

While R workers are required to complete their tasks in order to recover the AB product exactly, the completion of a *smaller* number of workers can be sufficient to approximate the AB product. For this approximation procedure, we next define a positive triple $(L_x, R_{x,l}, \tau_{x,l})$, for a CDC scheme of type-x. This triple specifies the number of resolution layers

(L_x), the approximate threshold ($R_{x,l}$), and the relative error ($\tau_{x,l}$) for the lth layer, where $l \in [L_x]$.

Definition 2 (Resolution layer): The resolution layer corresponds to a time index when a sufficient number of workers have completed their tasks so as to be able to generate an improved approximate of the AB product. For a CDC scheme of type-x, the parameter L_x with a subscript of its code type is used to refer to the number of resolution layers. The parameter L_x ranges between some minimum and maximum admissible values which will be detailed in Sec. III and IV. We list a summary of this notation in the third column of Table I.

Definition 3 (Approximate threshold): The approximate threshold is the number of workers required to approximate the AB product to some degree of accuracy. We denote the approximate threshold with $R_{x,l}$, where the first subscript x indicates the type of the code and l indicates the index of the resolution layer[3], which ranges from 1 to L_x. A summary of notation used for the approximate threshold of different CDC schemes is provided in the fourth column of Table I.

Definition 4 (Relative error): At layer $l \in [L_x]$, if the matrix $\tilde{C}_l \in \mathbb{R}^{N_x \times N_y}$ computes the approximate of the AB product, the relative error is defined as the Frobenius norm of the difference between $\tilde{C}_l$ and the exact AB product, normalized by the Frobenius norm of the matrix AB, i.e., $\|\tilde{C}_l - AB\|_F^2 / \|AB\|_F^2$. We use the notation $\tau_{x,l}$ with two subscripts (using similar logic to that of the approximation threshold) to refer to the relative error. We list the notation corresponding to the relative error in the last column of Table I.

Remark 1: Throughout this paper, we use the terms "exact" and "approximate" to differentiate between cases where the exact recovery of the AB product is possible or is not. We remark that in the situation of finite precision, even in the case of exact recovery, computation error is generally not identically zero due to numerical errors. Numerical error is of course not limited to exact recovery, it is also present in approximate recovery. In the next section, we detail a technique introduced in [13] to reduce issues of numerical precision. We use similar techniques to implement our methods in Sec. V.

C. Related Work for Benchmarking

Coefficient-based polynomial CDC schemes: MatDot codes [5] encode $\{A_k\}_{k=1}^{K}$ and $\{B_k\}_{k=1}^{K}$ to generate encoding polynomials as $\hat{A}(x) = \sum_{k=1}^{K} A_k x^{k-1}$ and $\hat{B}(x) = \sum_{k=0}^{K-1} B_{K-k} x^k$. The multiplication of $\hat{A}(x_n)$ and $\hat{B}(x_n)$ is assigned to worker $n \in [N]$, for an arbitrary real value of x_n (distinct from x_m for $m \neq n$). The decoding polynomial $\hat{A}(x)\hat{B}(x)$ for $x \in \{x_1, \ldots, x_N\}$ is a $(2K-2)$-degree polynomial, where the coefficient of x^{K-1} is equal to the target AB product. The completion of any $2K-1$ calculations of encoded products suffices to recover the entire polynomial, including the $(K-1)$th coefficient. We use $R_{MD} = 2K - 1$ to refer to the recovery threshold of MatDot codes. Note that $R_{MD} \leq N$. The recovery process of MatDot codes is an exact one. Either the AB product can be calculated exactly (once

---

[1]For any positive integer n, we use $[n]$ to refer to the set $\{1, \ldots, n\}$.

[2]We use the notations without their predetermined subscript code name in order to refer to a general code. For example, R refers to the recovery threshold of a general CDC scheme, while R_{MD} refers particularly to the recovery threshold of MatDot codes.

[3]Note that the recovery threshold is an extreme case of approximation threshold when the error is 0, so we use the same letter, although the subscripting is different.

CDC scheme	Recovery Thr.	# Resolution layers	Approx. Thr.	Rel. Err.
MatDot (MD) [5]	$R_{\mathrm{MD}} = 2K - 1$	0	–	–
ϵ-approximate MD [20]	$R_{\epsilon\mathrm{AMD}} = R_{\mathrm{MD}}$	1	$R_{\epsilon\mathrm{AMD},1} = K$	$\tau_{\epsilon\mathrm{AMD},1}$
OrthoMatDot [13]	$R_{\mathrm{OMD}} = R_{\mathrm{MD}}$	0	–	–
Lagrange [11]	$R_{\mathrm{Lag}} = R_{\mathrm{MD}}$	0	–	–
Group-wise SAC	$R_{\mathrm{G\text{-}SAC}} \geq R_{\mathrm{MD}}$	$L_{\mathrm{G\text{-}SAC}}$, $l \in [L_{\mathrm{G\text{-}SAC}}]$	$\{R_{\mathrm{G\text{-}SAC},l}\}_l$	$\{\tau_{\mathrm{G\text{-}SAC},l}\}_l$
Layer-wise SAC	$R_{\mathrm{L\text{-}SAC}} = R_{\mathrm{MD}}$	$L_{\mathrm{L\text{-}SAC}}$, $l \in [L_{\mathrm{L\text{-}SAC}}]$	$\{R_{\mathrm{L\text{-}SAC},l}\}_l$	$\{\tau_{\mathrm{L\text{-}SAC},l}\}_l$

any R_{MD} workers complete their tasks), or nothing can be said about AB (when fewer than R_{MD} workers have reported in).

Based on MatDot codes, ϵ-approximate MatDot codes [20] introduce an approximate recovery process. The strategy yields an approximation of the AB product when fewer than $2K-1$ workers have completed their tasks. In particular, when only $R_{\epsilon\mathrm{AMD},1} = K$ workers have completed their tasks, the AB product can be estimated with some error. The approximation is achieved by interpolating a $(K-1)$-degree polynomial $\hat{P}(x)$, where $\hat{P}(x)$ is the residual polynomial of the division of $\hat{A}(x)\hat{B}(x)$ by x^K. If we use $Q(x)$ to denote the quotient polynomial, then we can rewrite the decoding polynomial as $\hat{A}(x)\hat{B}(x) = x^K \hat{Q}(x) + \hat{P}(x)$, where $x^K\hat{Q}(x)$ consists of all higher-order terms and $\hat{P}(x)$ consists of all lower-order terms of $\hat{A}(x)\hat{B}(x)$ polynomial. Note that the leading coefficient (the coefficient of x^{K-1}) of $\hat{P}(x)$ is equal to the target $AB = \sum_{k=1}^{K} A_k B_k$ product and $\hat{A}(x)\hat{B}(x) \approx \hat{P}(x)$ if x is sufficiently small. The recovery procedure can be improved by an exact calculation of AB; possible once any $R_{\epsilon\mathrm{AMD}} = 2K-1$ workers finish their tasks and the $(2K-2)$-degree polynomial $\hat{A}(x)\hat{B}(x)$ can be interpolated.

Point-based polynomial CDC schemes: To address the problem of ill-conditioned Vandermonde matrices, OrthoMatDot codes are introduced in [13]. The key idea of OrthoMatDot codes is to use an *orthonormal* basis instead of the ill-conditioned monomial basis used in MatDot codes. An orthonormal basis is a system of algebraic polynomials, $\{O_k(x)\}$, with the degree of $O_k(x)$ equal to k for all $k = 0, 1, \ldots$. The polynomials are orthonormal on the interval $(-1, 1)$ with respect to a weight measure $w(x)$ [12]. In other words, for same nonnegative integrable function $w(x)$ in $(-1, 1)$, the inner products satisfy

$$\int_{1}^{-1} O_k(x) O_m(x) w(x) dx = \begin{cases} 1 & \text{if } k \neq m \\ 0 & \text{otherwise} \end{cases}.$$

For example, the Chebyshev polynomials are defined via a recursive formula [12]

$$\begin{cases} p_{k+1}(x) = 2x p_k(x) - p_{k-1}(x) & k = 1, 2, \ldots \\ p_0(x) = 1, \ p_1(x) = x \end{cases}.$$

The Chebyshev polynomials produce a well-known class of orthonormal polynomials; $O_0(x) = \frac{1}{\sqrt{2}} p_0(x)$, $O_k(x) = p_k(x)$, for $k = 1, 2, \ldots$ and $w(x) = \frac{2}{\pi\sqrt{1-x^2}}$. Using such an orthonormal polynomials (e.g., the Chebyshev polynomials), OrthoMatDot codes generate N pairs of encoding polynomials $(\tilde{O}_A(x_n), \tilde{O}_B(x_n))$, $n \in [N]$, from the $2K$ matrices $A_1, \ldots, A_K$ and $B_1, \ldots, B_K$. The encoding polynomials are $\tilde{O}_A(x) = \sum_{k=1}^{K} A_k O_k(x)$ and $\tilde{O}_B(x) = \sum_{k=1}^{K} B_k O_k(x)$. As before, worker $n \in [N]$ is tasked with the multiplication of $\tilde{O}_A(x_n)$ and $\tilde{O}_B(x_n)$, where $\{x_1, \ldots, x_N\}$ is a set of distinct real evaluation points. Since the decoding polynomial $\tilde{O}_A(x)\tilde{O}_B(x)$ is, in general, a $2K - 2$ degree polynomial, the recovery threshold of OrthoMatDot codes is equal to $R_{\mathrm{OMD}} = 2K - 1$. Assuming that the workers indexed by $j_1, \ldots, j_{2K-1}$ are the first to complete among all the N workers, the decoding procedure of OrthoMatDot codes involves a *Chebyshev-Vandermonde* matrix, defined as

$$\begin{pmatrix} O_0(x_{j_1}) & \cdots & O_0(x_{j_{2K-1}}) \\ \vdots & \ddots & \vdots \\ O_{2K-2}(x_{j_1}) & \cdots & O_{2K-2}(x_{j_{2K-1}}) \end{pmatrix}.$$

A careful choice of evaluation points, e.g., $x_n = \eta_n^{(N)}$, where $\{\eta_n^{(N)}\}$ are the N (distinct real) roots of $O_N(x)$, ensures that the Chebyshev Vandermonde system is well conditioned [13]. While well-conditioned, OrthoMatDot codes do require a post-decoding calculation in order to recover AB. Because the orthonormal basis is used, [13] proves that the AB product can be recovered via the sum $\sum_{k=1}^{K} \frac{2}{K} \tilde{O}_A(\eta_k^{(K)})\tilde{O}_B(\eta_k^{(K)})$, where the $\eta_k^{(K)}$ are the roots of $O_K(x)$.

Lagrange codes are another point-based polynomial CDC scheme originally introduced in [11]. Lagrange codes compute a general multivariate polynomial. In the following, we show how to apply Lagrange codes to our particular matrix multiplication problem. Lagrange codes encode data matrices $A_1, \ldots, A_K$ to generate the encoding polynomial as $\tilde{L}_A(x) = \sum_{k=1}^{K} A_k L_k(x)$, where $\{L_k(x)\}$ is Lagrange basis. Here, $L_k(x)$ is a $(K-1)$-degree polynomial, defined as $L_k(x) = \prod_{j \neq k} \frac{(x - y_j)}{(y_k - y_j)}$. Similarly, the encoding polynomial corresponding to data matrices $B_1, \ldots, B_K$ is $\tilde{L}_B(x) = \sum_{k=1}^{K} B_k L_k(x)$. Note that $\tilde{L}_A(y_k) = A_k$ and $\tilde{L}_B(y_k) = B_k$. The master assigns the multiplication of $\tilde{L}_A(x_n)$ and $\tilde{L}_B(x_n)$ to worker $n \in [N]$, where $x_1, \ldots, x_N$ are N distinct real numbers (possibly distinct from $\{y_k\}_{k \in [K]}$). Since each Lagrange polynomial $L_k(x)$ is of degree $K - 1$, the recovery threshold of Lagrange codes is $R_{\mathrm{Lag}} = 2K - 1$. When the polynomial $\tilde{L}_A(x)\tilde{L}_B(x)$ is ready for interpolation, Lagrange codes [11] solve a real-valued Vandermonde system of equations. After decoding, the $\tilde{L}_A(x)\tilde{L}_B(x)$ polynomial needs to be interpolated at K distinct interpolation points $y_1, \ldots, y_K$ and then summed together to recover the AB product, $AB = \sum_{k=1}^{K} \tilde{L}_A(y_k)\tilde{L}_B(y_k)$.

Remark 2: Among all above CDC schemes [5], [11], [13], [20], only ϵ-MatDot codes have a single resolution layer, i.e., $L_{\epsilon\text{AMD}} = 1$. All others support only an exact recovery process. They thus have no resolution layer.

III. GROUP-WISE SUCCESSIVE APPROXIMATED CODING

In this section, we introduce group-wise SAC. Our method extends the single-layer approximation procedure of ϵ-approximate MatDot codes [20] to multiple resolution layers. The recovery process of group-wise SAC consists of multiple resolution layers before exact recovery. This enables successive improvements of the approximations of the AB product as additional workers report in. While such successive improvements are (marginally) obtained whenever an additional resolution layer completes, the major improvements of group-wise SAC occur once groups of layers complete. We next detail our constructions.

In group-wise SAC, we divide the resolution layers into D (disjoint and consecutive) groups. Group $d \in [D]$ contains L_d layers. The total number of layers is $L_{\text{G-SAC}} = \sum_{d=1}^{D} L_d$. The approximation of the AB product that is obtained in layer $l_{d,i}$, $d \in [D]$ and $i \in [L_d]$, improves as either d or i increases. Resolution increases in discrete steps when d increments but only slightly as l increments. To explain better, consider the first resolution layer of the dth group (layer $l_{d,1} = 1 + \sum_{j=1}^{d-1} L_j$). This layer provides an approximation of significantly higher resolution than earlier layers (layers in the $(d-1)$th group). On the other hand, in the same group d, layer $l_{d,i}$ approximates AB only slightly better than the previous layer, $l_{d,i-1}$. We next provide the approximate threshold required for each of these resolution layers.

In layer $l \in [L_{\text{G-SAC}}]$, the approximate threshold is $R_{\text{G-SAC},l}$. I.e., our method approximates the AB product when $R_{\text{G-SAC},l}$ workers have completed their tasks. While in ϵ-approximate MatDot codes [20] the approximate threshold is K, our group-wise SAC allows the approximate threshold of the first layer to be any arbitrary (integer) value less than or equal to K, i.e., $R_{\text{G-SAC},1} \le K$. As more workers complete tasks, the initial resolution can be improved. Across resolution layers $l \in \{2, 3, \ldots, L_{\text{G-SAC}}\}$, our method is designed in such a way that the approximate thresholds satisfy $R_{\text{G-SAC},l} = R_{\text{G-SAC},l-1} + 1$ (cf. Secs. III-A and III-B for details of this design). Finally, our method recovers the exact AB product when a sufficient number of workers (larger than or equal to $2K - 1$) complete their tasks. In other words, the recovery threshold of our group-wise SAC satisfies $R_{\text{G-SAC}} \ge 2K - 1$. Therefore, one can conclude that $L_{\text{G-SAC}} \in \{R_{\text{G-SAC}} - K, \ldots, R_{\text{G-SAC}} - 1\}$ (see App. A for proof). Next, to develop the basic ideas in Sec. III-A, we detail group-wise SAC for $D = 2$ groups. We call this *two-group* SAC. We generalize to *multi-group* SAC in Sec. III-B.

A. Two-Group SAC

We now introduce two-group SAC. We use MatDot codes [5] to generate encoding polynomials $\hat{S}_A(x)$ and $\hat{S}_B(x)$ for two-group SAC. However, the two $(K-1)$-degree polynomials $\hat{S}_A(x)$ and $\hat{S}_B(x)$ are different from the encoding polynomials $\hat{A}(x)$ and $\hat{B}(x)$, used in the $\epsilon-$approximate MatDot code design detailed in Sec. II-C. The coefficients of $\hat{S}_A(x)$ and $\hat{S}_B(x)$ are the permuted version of the coefficients of $\hat{A}(x)$ and $\hat{B}(x)$, respectively. To permute the coefficients, we *uniformly* shuffle the pairs of submatrices $(A_1, B_1), \ldots, (A_K, B_K)$ to get $(A_{i_1}, B_{i_1}), \ldots, (A_{i_K}, B_{i_K})$ and then divide the latter into two groups. The first group consists of the first $K_1 = R_{\text{G-SAC},1}$ pairs $(A_{i_1}, B_{i_1}), \ldots, (A_{i_{K_1}}, B_{i_{K_1}})$. The other $K_2 = K - K_1$ pairs belong to the second group. We generate encoding polynomials as

$$\hat{S}_A(x) = \left(\sum_{k=1}^{K} A_{i_k} x^{k-1} \right) \text{ and}$$

$$\hat{S}_B(x) = \left(\sum_{k=0}^{K_1-1} B_{i_{K_1-k}} x^k \right) + \left(\sum_{k=0}^{K_2-1} B_{i_{K-k}} x^{K_1+k} \right).$$

The master assigns the multiplication of $\hat{S}_A(x_n)$ and $\hat{S}_B(x_n)$ to worker $n \in [N]$. Once sufficient numbers of workers complete their tasks, the master first approximates the AB product through $L_{\text{G-SAC}} = L_1 + L_2$ resolution layers and finally recovers the exact AB. This can be explained as follows. Note that in two-group SAC, $L_1 = K$, $L_2 = K_2 - 1$ if $K_2 > 0$ and equals 0 otherwise. We also note that the matrix product $\hat{S}_A(x) \hat{S}_B(x)$ is a $(2K-2)$-degree polynomial. In the lth resolution layer, $l \in [L_{\text{G-SAC}}]$, $\hat{S}_A(x) \hat{S}_B(x)$ can be written as a sum of a $(l + K_1 - 2)$-degree polynomial $\hat{P}_l(x)$ and the polynomial $x^{l+K_1-1} \hat{Q}_l(x)$ of higher-order terms. I.e., $\hat{S}_A(x) \hat{S}_B(x) = x^{l+K_1-1} \hat{Q}_l(x) + \hat{P}_l(x)$. Similar to ϵ-approximate MatDot codes, by setting the evaluation points $x_1, \ldots, x_N$ to be distinct and (sufficiently) small, we are able to approximate $\hat{P}_l(x_n)$ by $\hat{S}_A(x_n) \hat{S}_B(x_n)$ for any $n \in [N]$. We next detail the basic ideas of how to approximate AB starting from the first resolution layer.

In the first resolution layer, once the fastest $R_{\text{G-SAC},1} = K_1$ workers complete their tasks, the master *approximately* interpolates $\hat{P}_1(x)$ to recover the leading coefficient, $\sum_{k=1}^{K_1} A_{i_k} B_{i_k}$, to some accuracy. Define $C := AB$ and $C_l := \sum_{k=1}^{m_l} A_{i_k} B_{i_k}$. For the first layer, $l = 1$ and $m_1 = K_1$. In the following theorem, we show how optimally to select a scaling β such that βC_l is a good estimate of C. We start from the *expected approximation error*, defined as $\mathbb{E}\left(\|C - \beta C_l\|_F^2 \right)$, where the expectation is taken with respect to the indices of the random permutation of the (A_i, B_i) pairs. The proof of the following theorem is provided in App. B.

Theorem 1: For a uniform random permutation of the (A_i, B_i) pairs, the optimum solution to $\arg\min_\beta \mathbb{E}\left(\|C - \beta C_l\|_F^2 \right)$ is

$$\beta^* = \frac{M_1 + 2M_2}{M_1 + 2\frac{(m_l-1)}{(K-1)}M_2}, \tag{1}$$

where

$$M_1 = \sum_{i=1}^{K} \|A_i B_i\|_F^2 \text{ and } M_2 = \sum_{i,j=1, i<j}^{K} \text{Tr}\left((A_i B_i)^T (A_j B_j) \right).$$

Remark 3: We note that in general, neither M_1 nor M_2 will be known because they depend on the $A_k B_k$ products which

are the constituent computations we want. We note that while setting $\beta = \frac{K}{m_l}$ makes βC_l an unbiased estimate of C (see Eq. (10) in App. B), that choice for β does not necessarily minimize the expected approximation error.

Remark 4: While the optimal choice of β will not in general be known, one can approximate it in the following two cases:

- *Case 1:* The β^* is approximately equal to 1 if M_2 is small compared to M_1. While in general we cannot check whether or not this condition holds, prior knowledge of the distributions of A_i and B_i matrices can help us to conclude when this condition will be likely to hold. For example, if the entries of A_i, A_j, B_i and B_j are independent and identically distributed (i.i.d) random variables of zero mean and high variance then, in expectation, $\mathrm{Tr}\left((A_iB_i)^T(A_jB_j)\right)$ is zero if $i \neq j$ and is nonzero if $i = j$. This implies that $\mathbb{E}(M_2) = 0$ and $\mathbb{E}(M_1) \neq 0$, and thus β^* is highly likely to be close to unity.

- *Case 2:* In another extreme, if $M_1 \ll M_2$, then the optimal $\beta^* \approx \frac{K-1}{m_l-1}$. In this case, the optimal β^* is close to $\frac{K}{m_l}$ which per the earlier remark is an unbiased estimate. Similar to Case 1, the condition $M_1 \ll M_2$ is quite likely to hold in certain situations. For example, consider a situation where the entries $(A_i)_{e,k}$ and $(A_j)_{e,k}$ in any two matrices A_i and A_j, $i \neq j$, are strongly and positively correlated, and the entries of B_i and B_j are also strongly and positively correlated. If the entries of the A_i and B_i are independent and have zero mean, then $\mathbb{E}(M_2)$ is a sum of $\binom{K}{2}$ large positive terms, while $\mathbb{E}(M_1)$ is a sum of only K terms. Since the former has $\mathcal{O}(K)$ more large terms than the later, with a high probability $M_1 \ll M_2$ and $\beta^* \approx \frac{K-1}{m_l-1}$.

Now, we generalize the approximation procedure of AB to any resolution layer $l \in [L_{\text{G-SAC}}]$. In layer $l \in [L_{\text{G-SAC}}]$, when $R_{\text{G-SAC},l} = l + K_1 - 1$ workers complete their tasks, the polynomial $\hat{P}_l(x)$ can be interpolated to some accuracy. The coefficient of x^{K_1-1} in $\hat{P}_l(x)$ is equal to $\sum_{k=1}^{K_1} A_{i_k} B_{i_k}$ which can be used to approximate AB. When $K_1 < K$, $\sum_{k=1}^{K_1} A_{i_k} B_{i_k}$ is the sum of only a subset of outer products rather than all the outer products. Using the same notation as Thm. 1, we use C_l to denote the partial sum $\sum_{k=1}^{K_1} A_{i_k} B_{i_k}$ and make m_l equal to K_1 for the first L_1 resolution layers (i.e., for $l \in [L_1]$). Note that $\hat{S}_A(x)\hat{S}_B(x)$ estimates $\hat{P}_l(x)$ more accurately than does $\hat{P}_{l-1}(x)$ because $\hat{P}_l(x)$ contains more terms of the $\hat{S}_A(x)\hat{S}_B(x)$ polynomial. This leads to the gradual improvement (in expectation) in the resolution of C_l as l increases from 1 to L_1.

If l exceeds L_1, either the exact recovery is enabled (if $L_2 = 0$) or the resolution layer $l = L_1 + 1$ approaches (if $L_2 > 0$). In either case, $C_{L_1+1} = \sum_{k=1}^{K} A_{i_k} B_{i_k}$ can be computed to some accuracy which yields a strictly better resolution of the full summation. In the case of $L_2 > 0$, as l increases from $L_1 + 1$ to $L_{\text{G-SAC}}$, the resolution of $C_l = \sum_{k=1}^{K} A_{i_k} B_{i_k}$ is gradually improved (in expectation). When $K_1 = K$, our method is similar to ϵ-approximate MatDot codes in the sense that the master needs to wait for the same number of workers ($R_{\text{G-SAC},1} = K$) to provide the first approximation of AB. However, in this case, our method still

outperforms ϵ-approximate coding to some degree because the master can gradually improve on this resolution prior to exact recovery as l increases from 1 to $L_{\text{G-SAC}}$.

Lastly, when any $R_{\text{G-SAC}} = 2K - 1$ workers complete their tasks, the master is able to interpolate the $\hat{S}_A(x)\hat{S}_B(x)$ polynomial exactly and recover its coefficients. When $K_1 < K$, the coefficient of x^{K_1-1} is equal to $\sum_{k=1}^{K_1} A_{i_k} B_{i_k}$ and the coefficient of x^{K+K_1-1} is equal to $\sum_{k=K_1+1}^{K} A_{i_k} B_{i_k}$. The summation of these two coefficients yields the AB product without approximation error. When $K_1 = K$, only the coefficient of the x^{K_1-1} term is required because it is equal to the full summation $\sum_{k=1}^{K} A_{i_k} B_{i_k}$.

Example 1 (Two-group SAC): In Fig. 1(a,b), a motivating example benchmarks our two-group SAC against ϵ-approximate MatDot codes [20] (ϵAMD), where $K = 8$. Each subfigure is an array that consists of 8 rows and 8 columns. In Fig. 1(a) which presents the ϵAMD codes, each row $i \in [8]$ corresponds to the coefficient of x^{i-1} in the encoding polynomials $\hat{A}(x)$. This coefficient is assumed to be equal to the submatrix A_i. Similarly, the ith column corresponds to the B_{9-i} submatrix. As a result, the (i,j)th intersection corresponds to the product of the ith and jth coefficients in $\hat{A}(x)$ and $\hat{B}(x)$, respectively. Note that the arrays consist of 15 antidiagonals (a diagonal from the top right to the bottom left). The summation of all coefficients along on each antidiagonal is equal to one of the coefficients in the decoding polynomial. For example, in Fig. 1(a), the sum of coefficients in the 8 solid boxes of the main antidiagonal is the coefficient of x^7 in $\hat{A}(x)\hat{B}(x)$, equal to $AB = \sum_{i=1}^{8} A_i B_i$.

On the other hand, Figure 1(b) presents the two-layer SAC where the ith column corresponds to B_{6-i} if $i < 6$ and corresponds to B_{14-i} otherwise. This can be justified via the difference in the encoding procedures of two-group SAC and ϵAMD which is due to the coefficient of x^{i-1}, $i \in [8]$, in $\hat{S}_B(x)$ and $\hat{B}(x)$. In Fig. 1(b), the summation of coefficients in the hatched boxes is the coefficient of x^4 in the $\hat{S}_A(x)\hat{S}_B(x)$ polynomial. This is equal to $\sum_{i=1}^{5} A_i B_i \approx AB$. The summation of coefficients in the grid boxes is the coefficient of x^{12}, equal to $\sum_{i=6}^{8} A_i B_i$. This can be summed with $\sum_{i=1}^{5} A_i B_i$ to recover the exact AB product.

While in Fig. 1(a), the master needs to wait for $R_{\epsilon\text{AMD},1} = 8$ completed workers to provide an estimate of AB, in Fig. 1(b), the master only needs to wait for $R_{\text{G-SAC},1} = 5$ workers to provide an initial relatively low resolution. It then can gradually improve this resolution as l increases from 1 to 8. Once $R_{\text{G-SAC},9} = 13$ workers have completed their tasks, the master provides another relatively high resolution. It can improve this resolution slightly at $l = L_{\text{G-SAC}} = 10$. In both Figs. 1(a,b), the master recovers the exact AB product, once any $R_{\epsilon\text{AMD}} = R_{\text{G-SAC}} = 15$ workers complete.

B. Multi-Group SAC

We now generalize two-group SAC to multiple groups. Similar to two-group SAC, we uniformly shuffle the pairs of submatrices so that $i_1, \ldots, i_K$ refer to the indices of the shuffled pairs, i.e., $(A_{i_1}, B_{i_1}), \ldots, (A_{i_K}, B_{i_K})$. As noted before, the reason that we use uniform shuffling is to provide improved
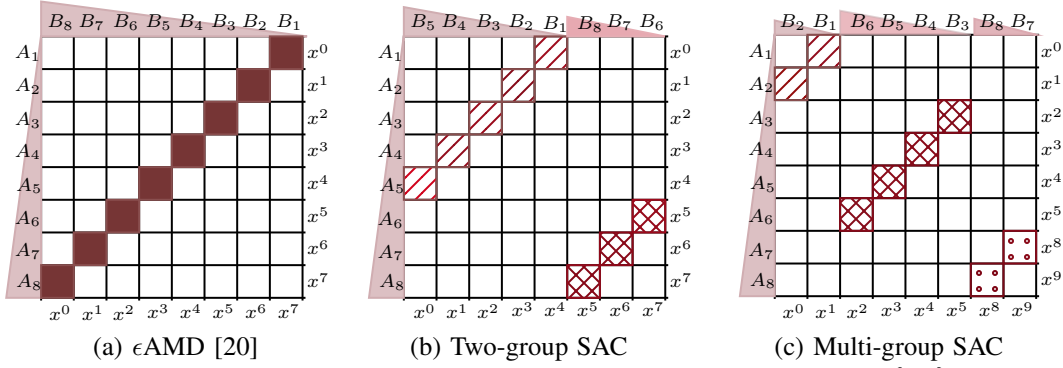
Fig. 1. Motivating examples for ϵ-approximate MatDot coding and its successive designs. In (a) $K = 8$, in (b) $K_i \in \{5, 3\}$, and in (c) $K_i \in \{2, 4, 2\}$.

estimate of AB (in expectation) as more workers report in. We divide these shuffled pairs into $D \geq 2$ groups. The dth group consists of K_d pairs $(A_{i_{k+\sum_{j=1}^{d-1} K_j}}, B_{i_{k+\sum_{j=1}^{d-1} K_j}})$, $k \in [K_d]$. Thus, $\sum_{d=1}^{D} K_d = K$. For simplicity of notation, we use $(A_k^{(d)}, B_k^{(d)})$ to refer to the pair $(A_{i_{k+\sum_{j=1}^{d-1} K_j}}, B_{i_{k+\sum_{j=1}^{d-1} K_j}})$, for all $k \in [K_d]$ and $d \in [D]$. We encode matrices as

$$\hat{S}_A(x) = \left(\sum_{k=1}^{K_1} A_k^{(1)} x^{k-1}\right) + x^{K_1} \left(\sum_{k=1}^{K_2} A_k^{(2)} x^{k-1}\right)$$
$$+ \sum_{d=3}^{D} \left(x^{g(d)} \left(\sum_{k=1}^{K_d} A_k^{(d)} x^{k-1}\right)\right) \text{ and}$$

$$\hat{S}_B(x) = \left(\sum_{k=0}^{K_1-1} B_{K_1-k}^{(1)} x^k\right) + x^{K_1} \left(\sum_{k=0}^{K_2-1} B_{K_2-k}^{(2)} x^k\right)$$
$$+ \sum_{d=3}^{D} \left(x^{g(d)} \left(\sum_{k=0}^{K_d-1} B_{K_d-k}^{(d)} x^k\right)\right),$$

where $g(d) = K_1 + \left(\sum_{j=3}^{d} \left(\left(\sum_{i=1}^{j-2} 2^{j-i-2} K_i\right) + K_{j-1}\right)\right)$ for $d \geq 3$. Next, worker $n \in [N]$ multiplies $\hat{S}_A(x_n)$ and $\hat{S}_B(x_n)$ for sufficiently small value of x_n (x_n and $x_{n'}$ are distinct if $n \neq n'$). The decoding polynomial $\hat{S}_A(x)\hat{S}_B(x)$ has degree $(\sum_{d=1}^{D} 2^{D-d} K_d) + K_D - 2$. Therefore, in the exact recovery layer, the recovery threshold is equal to $R_{\text{G-SAC}} = (\sum_{d=1}^{D} 2^{D-d} K_d) + K_D - 1$. If $D = 2$, this recovery threshold is equal to that of two-group SAC, while if $D > 2$, $R_{\text{G-SAC}} > 2K - 1$ (cf. App. E for proofs of these claims). In group $d \in [D]$, whenever any $R_{\text{G-SAC},l_{d,1}} = \sum_{i=1}^{d} 2^{d-i} K_i$ workers complete their tasks, the master can interpolate the $(R_{\text{G-SAC},l_{d,1}}-1)$−degree polynomial $\hat{P}_{l_{d,1}}(x)$. This polynomial consists of all terms that have lower order than $x^{R_{\text{G-SAC},l_{d,1}}}$ in the $\hat{S}_A(x)\hat{S}_B(x)$ polynomial. This means that we can expand $\hat{S}_A(x)\hat{S}_B(x)$ as $\hat{P}_{l_{d,1}}(x) + x^{R_{\text{G-SAC},l_{d,1}}} \hat{Q}_{l_{d,1}}(x)$. The leading coefficient of $\hat{P}_{l_{d,1}}(x)$ is equal to $\sum_{i=1}^{K_d} A_i^{(d)} B_i^{(d)}$ which when summed with the earlier estimates of $\sum_{i=1}^{K_1} A_i^{(1)} B_i^{(1)}, \ldots, \sum_{i=1}^{K_{d-1}} A_i^{(d-1)} B_i^{(d-1)}$, yields (in expectation) a better estimate of the AB product. In the group $d \in [D]$, the layer $j \in \{2, \ldots, L_d\}$ enables the interpolation of the $\hat{P}_{l_{d,j}}(x)$ polynomial which has degree $R_{\text{G-SAC},l_{d,j}} - 1 = R_{\text{G-SAC},l_{d,1}} + j - 2$. This interpolation while leading to a better estimate of $\sum_{i=1}^{K_1} A_i^{(1)} B_i^{(1)}, \ldots, \sum_{i=1}^{K_d} A_i^{(d)} B_i^{(d)}$, does not provide any

new estimates of the product of the remaining pairs. Therefore, its estimate improves only slightly as j increases within the dth group.

Example 2 (Multi-group SAC): In Fig. 1(c), we depict an example of Multi-group SAC, where $D = 3$. Similar to Figs. 1(a,b), we set $K = 8$ for a fair comparison. For illustrative reasons, we set other parameters as $K_d \in \{2, 4, 2\}$, $L_{\text{G-SAC}} = 17$, $R_{\text{G-SAC},d} \in \{2, \ldots, 18\}$, and $R_{\text{G-SAC}} = 19$. Compared to Example. 1, we have $R_{\text{G-SAC},1} < 5$ and $15 < R_{\text{G-SAC}}$. In Fig. 1(c), the hatched boxes correspond to the first group of pairs: (A_1, B_1) and (A_2, B_2). Similarly, the grid and dotted boxes, respectively, correspond to the second and third groups of pairs. The summation of coefficients in these three groups respectively yields $\sum_{i=1}^{2} A_i B_i$, $\sum_{i=3}^{6} A_i B_i$, and $\sum_{i=7}^{8} A_i B_i$. Compared to the arrays in Fig. 1(a,b), not only the ith column ($i \in [8]$) of the array in Fig. 1(c) corresponds to a different submatrix of B, but also the ith row and column do *not* always correspond to the coefficient of x^{i-1}. For example, in Fig. 1(c), the 7th and 8th rows correspond to the coefficients of x^8 and x^9 in $\hat{S}_A(x)$.

Note that this choice of polynomials in generating $\hat{S}_A(x)$ and $\hat{S}_B(x)$ allows us to recover the summation of only a subset of antidiagonals in our multi-group SAC. For example, consider the grid boxes in Fig. 1(c). Although there exist four other boxes in the main antidiagonal, corresponding to the products $A_1 B_7$, $A_2 B_8$, $A_7 B_1$, and $A_8 B_2$, the coefficient of $x^{R_{\text{G-SAC},7}-1}$ in the polynomial $\hat{S}_A(x)\hat{S}_B(x)$ is equal to the summation of the $A_i B_i$ products only for $i \in \{3, 4, 5, 6\}$ (depicted with grid boxes on the main antidiagonal). This benefit is achieved at the cost of increasing the degree of the polynomial $\hat{S}_A(x)\hat{S}_B(x)$. While in $\hat{A}(x)\hat{B}(x)$ and $\hat{S}_A(x)\hat{S}_B(x)$ have degree 15, the degree of polynomial $\hat{S}_A(x)\hat{S}_B(x)$ is equal to 18. This increased degree delays the exact recovery of AB.

IV. LAYER-WISE SUCCESSIVE APPROXIMATED CODING

In this section, we extend our successive approximated coding (SAC) to point-based CDC schemes including OrthoMat-Dot [13] and Lagrange [11] codes. To accomplish this, we select a specific set of evaluation points for workers to evaluate the polynomial at, different from the evaluation points used by point-based CDC schemes. Evaluating the polynomials at the elements of this specific set allows the master to approximate AB starting from the evaluation of the fastest worker and continuously reducing the error as more workers report in. This continuity of approximation procedure in layer-wise SAC is in

contrast to the approximation procedure of group-wise SAC, where the master realizes significant improvements in estimate quality only when each additional group of workers completes their tasks. In the following, we first detail our layer-wise SAC in terms of a general point-based CDC scheme. We then develop two specific constructions, one using OrthoMatDot [13], the other Lagrange codes [11].

A. Layer-wise SAC for Point-based CDC

We now introduce our layer-wise SAC which is applied to point-based CDC. Before doing so, we first formulate a general framework for point-based CDC. This framework unifies existing point-based methods ([11], [13]) and motivates new techniques[4]. We consider a polynomial basis $\{T_k(x)\}$, where the maximum degree of the first K polynomials (i.e., $T_0(x), \ldots, T_{K-1}(x)$) is $K - 1$. We use this basis to encode the $2K$ matrices $A_1, \ldots, A_K$ and $B_1, \ldots, B_K$. We generate encoding polynomials as $\tilde{S}_A(x) = \sum_{k=1}^{K} A_k T_{k-1}(x)$ and $\tilde{S}_B(x) = \sum_{k=1}^{K} B_k T_{k-1}(x)$. Since the degree of each $\tilde{S}_A(x)$ and $\tilde{S}_B(x)$ polynomial is (at most, and typically, is equal to) $K - 1$, the degree of the decoding polynomial $\tilde{S}_A(x)\tilde{S}_B(x)$ is $2K - 2$. The master assigns the multiplication of $\tilde{S}_A(x_n)$ and $\tilde{S}_B(x_n)$ to worker $n \in [N]$, where $x_n \neq x_{n'}$ for $n \neq n'$. This task equates to evaluating the decoding polynomial at a single point. In point-based CDC, each evaluation point is selected from a set of N distinct real numbers, denoted $\mathcal{X}_{\text{pt-based}}$. Once workers provide the evaluation of the $\tilde{S}_A(x)\tilde{S}_B(x)$ polynomial at any $2K - 1$ (distinct) points, it can be fully decoded (e.g., via the Vandermonde systems of equations). After decoding, a two-step post-decoding calculation is required to recover AB. In the first step, the decoding polynomial $\tilde{S}_A(x)\tilde{S}_B(x)$ is interpolated at a new set of points. At the second step, these new interpolated results are linearly combined to recover AB. For simplicity of applying the notation to prior point-based CDC schemes ([11], [13]), we assume that the $\tilde{S}_A(x)\tilde{S}_B(x)$ polynomial needs to be calculated at only K interpolation points $\{y_k\}_{k=1}^{K}$ in the first step. Then, the desired computation can be recovered via the sum $\sum_{k=1}^{K} \alpha_k \tilde{S}_A(y_k)\tilde{S}_B(y_k)$, where α_k are scalar coefficients determined by y_k.

Building on the point-based CDC construction, our layer-wise SAC adds $L_{\text{L-SAC}} = 2K - 2$ resolution layers before exact recovery. In other words, starting from the moment that the fastest worker completes its task, the master is able (with error) to estimate $\sum_{k=1}^{K} \alpha_k \tilde{S}_A(y_k)\tilde{S}_B(y_k)$. The master can (in expectation) improve its estimate as more workers complete jobs. In layer-wise SAC, the master generates the same pair of polynomials $(\tilde{S}_A(x), \tilde{S}_B(x))$ as in point-based CDC schemes. However, in contrast to point-based CDC schemes which use evaluations points $x \in \mathcal{X}_{\text{pt-based}}$, in layer-wise SAC we use a different set of evaluation points, denoted $\mathcal{X}_{\text{L-SAC}}$. In particular, $\mathcal{X}_{\text{L-SAC}} = \{z_{k,i}\}_{k \in [K], i \in [n_k]}$, where $\sum_{k=1}^{K} n_k = N$, and for any $k \in [K]$, the $z_{k,1}, \ldots, z_{k,n_k}$ are n_k distinct real numbers "ϵ-close" to y_k. For any $i \in [n_k]$, y_k and $z_{k,i}$ are "ϵ-close" if

---

[4]We note that while current works on point-based CDC use either Orthonormal or Lagrange basis, the extension of point-based CDC to other polynomial bases can be considered for future work.

and only if $|y_k - z_{k,i}| \leq \epsilon$. With this definition, $z_{k,i}$ and $z_{k,j}$ are 2ϵ-close. Next, we explain the reason for this selection.

To describe the decoding process, we sort workers according to their speed. We index the workers as $j_1, \ldots, j_N$ so that worker j_1 is the fastest and worker j_N is the slowest. At resolution layer $m \in [L_{\text{L-SAC}}]$, the m fastest workers, corresponding to indices $j_1, \ldots, j_m$ have completed their tasks. We use $\{x_{j_1}, \ldots, x_{j_m}\}$ to denote the set of evaluation points assigned to the m fastest workers. Let's assume that this set includes m_k (distinct) elements of $\{z_{k,i}\}_{i \in [n_k]}$ for each $k \in [K]$. In other words, for any $k \in [K]$, there exists (distinct) indices $j_{k,1}, \ldots, j_{k,m_k}$ such that $\{x_{j_1}, \ldots, x_{j_m}\} = \bigcup_{k=1}^{K} \{z_{k,j_{k,1}}, \ldots, z_{k,j_{k,m_k}}\}$; m_k must satisfy $\sum_{k=1}^{K} m_k = m$ and $0 \leq m_k \leq n_k$. From the tasks that are completed by the m fastest workers, we define

$$\tilde{C}_m = \sum_{k=1}^{K} \alpha_k \frac{\sum_{i=1}^{m_k} \tilde{S}_A(z_{k,j_{k,i}})\tilde{S}_B(z_{k,j_{k,i}})}{m_k}. \quad (2)$$

In limit, since polynomials are continuous

$$\lim_{\epsilon \to 0} \tilde{C}_m = C_m := \sum_{k=1}^{K} \alpha_k \tilde{S}_A(y_k)\tilde{S}_B(y_k) \mathbb{1}_{m_k > 0}, \quad (3)$$

where $\mathbb{1}_{m_k > 0}$ is an indicator function, equals 1 if $m_k > 0$, and 0 otherwise (for detailed proof see App. D). In the following theorem, we show how to estimate AB using C_m.

Theorem 2: If the order of completion is uniform over all permutation, the optimal choice of β that minimizes the expected approximation error, $\mathbb{E}\left(\|C - \beta C_m\|_F^2\right)$, where the expectation is taken with respect to random variables m_k, is

$$\beta^* = \frac{\left(\sum_{i=1}^{K} \tilde{M}_i \gamma_i\right) + \left(\sum_{i,j=1, i<j}^{K} \tilde{M}_{i,j}(\gamma_i + \gamma_j)\right)}{\left(\sum_{i=1}^{K} \tilde{M}_i \gamma_i\right) + 2\left(\sum_{i,j=1, i<j}^{K} \tilde{M}_{i,j}\gamma_{i,j}\right)}, \quad (4)$$

where

$$\tilde{M}_i = \alpha_i^2 \|\tilde{S}_A(y_i)\tilde{S}_B(y_i)\|_F^2,$$

$$\tilde{M}_{i,j} = \alpha_i \alpha_j \text{Tr}\left(\left(\tilde{S}_A(y_i)\tilde{S}_B(y_i)\right)^T \left(\tilde{S}_A(y_j)\tilde{S}_B(y_j)\right)\right),$$

$$\gamma_i = \frac{\binom{N}{m} - \binom{N-n_i}{m}}{\binom{N}{m}}, \text{ and}$$

$$\gamma_{i,j} = \frac{\binom{N}{m} - \binom{N-n_i}{m} - \binom{N-n_j}{m} + \binom{N-n_i-n_j}{m}}{\binom{N}{m}}.$$

The proof of this theorem is provided in App. C.

Remark 5: As in Thm. 1, $\tilde{M}_i$ and $\tilde{M}_{i,j}$ are not known a priori. Furthermore, it is not always possible to approximate β^* in a manner similar to how we did in cases 1 and 2 in Remark. 4. This is because in contrast to group-wise SAC where resolution layers yield a partial sum of the $A_i B_i$ products, in layer-wise SAC (which applies to point-based CDC), C_m is a function of the $\tilde{S}_A(y_i)\tilde{S}_B(y_i)$ rather than of the $A_i B_i$. Therefore, since the calculation of $\tilde{M}_i$ and $\tilde{M}_{i,j}$ require evaluations of the $\tilde{S}_A(y_i)\tilde{S}_B(y_i)$ products, even with prior knowledge of the distributions of $A_i B_i$, it is not apparent how to approximate β^*. However, for specific point-based polynomials where $\tilde{S}_A(y_i)\tilde{S}_B(y_i) = A_i B_i$, we can

approximate β^* when layer-wise SAC is applied to. As an example, in the next section we will show how to approximate β^* in Lagrange layer-wise SAC.

B. Examples

We now provide examples that apply our layer-wise SAC to two specific point-based CDC schemes: OrthoMatDot [13] and Lagrange [11] codes.

Example 3 (Layer-wise SAC via OrthoMatDot codes): For a fair comparison, we set $K = 8$ as in Examples 1 and 2. In this example, the master uses orthonormal polynomial basis $\{O_k(x)\}$ to generate the 7-degree encoded polynomials via $\tilde{S}_A(x) = \sum_{k=1}^{8} A_k O_k(x)$ and $\tilde{S}_B(x) = \sum_{k=1}^{8} B_k O_k(x)$. For illustrative reasons, we assume that $\frac{N}{8} \in \mathbb{Z}$. The master divides N workers into K equally sized groups so that $n_k = N/K$ for all $k \in [8]$. It then produces the $N/8$ pairs of polynomials $(\tilde{S}_A(z_{k,1}), \tilde{S}_B(z_{k,1})), \ldots, (\tilde{S}_A(z_{k,N/8}), \tilde{S}_B(z_{k,N/8}))$, and distributes them to the $N/8$ workers of group $k \in [8]$. For all $i \in [N/8]$, $z_{k,i}$ is ϵ-close to $\eta_i^{(8)}$. Recall from Sec. II-C, $\eta_1^{(8)}, \ldots, \eta_8^{(8)}$ are the 8 roots of $O_8(x)$. Note that since the set $\mathcal{X}_{\text{L-SAC}} = \{z_{k,i}\}$ differs from the evaluation set used by OrthoMatDot codes ($\mathcal{X}_{\text{OMD}} = \{\eta_n^{(N)}\}$), our method cannot benefit from Chebyshev Vandermonde interpolation as much as OrthoMatDot codes can in the exact recovery layer.

However, on the positive side, our Layer-wise SAC enables $L_{\text{L-SAC}} = 14$ resolutions before exact recovery. Since $\tilde{S}_A(x)\tilde{S}_B(x)$ is a degree-14 polynomial, the recovery threshold is $R_{\text{L-SAC}} = 15$, equal to that of Example 1 and is less than $R_{\text{G-SAC}}$ in Example 2. As noted earlier, layer-wise SAC provides estimates of AB that continuously improve in accuracy as workers complete tasks. This is in contrast to group-wise SAC. In Example 1, relatively discrete steps in error reduction occur at layers $l = 1$ and $l = 9$. In Example 2, such steps occur at layers $l = 1, 7$, and 17.

Example 4 (Layer-wise SAC via Lagrange codes): In contrast to the previous example that uses an orthonormal basis, we now extend layer-wise SAC to Lagrange codes which use the Lagrange basis $\{L_k(x)\}$. As before, let $K = 8$ and set $n_k = N/8$ for all $k \in [8]$. In this example, our method generates encoding polynomials that are similar to those of Lagrange codes: $\tilde{S}_A(x) = \sum_{k=1}^{8} A_k L_k(x)$ and $\tilde{S}_B(x) = \sum_{k=1}^{8} B_k L_k(x)$. However, in layer-wise SAC, these polynomials are evaluated at $\mathcal{X}_{\text{L-SAC}} = \{y_{k,i}\}$, where $y_{k,i}$ is ϵ−close to y_k for $i \in [N/8]$ and $k \in [8]$. Similar to Example 3, when layer-wise SAC method applies to Lagrange codes, it provides its first estimate when the first worker completes its task (note $R_{\text{L-SAC},1} = 1$). Layer-wise SAC then continuously improves its estimate as l increases from 2 to 14. Layer-wise SAC recovers the exact AB product once $R_{\text{L-SAC}} = 15$ workers complete their tasks.

There are some differences between Examples 3 and 4. In addition to the use of different polynomial bases and different evaluation points, in Example 4 the AB product can be recovered by simply computing the sum $\sum_{k=1}^{K} \tilde{S}_A(y_k)\tilde{S}_B(y_k)$. I.e., in Example 4 the kth scalar coefficient equals $\alpha_k = 1$. However, in Example 3, $\tilde{S}_A(y_k)\tilde{S}_B(y_k)$ should first be scaled

by $\frac{2}{K}$ and then summed. Furthermore, in contrast to Example 3, the evaluation of $\tilde{S}_A(y_k)\tilde{S}_B(y_k)$ in Example 4 results in the $A_k B_k$ matrix product. Therefore, with prior knowledge of the distributions of $A_k B_k$, we can approximate β^* in Lagrange layer-wise SAC. Similar to Remark 4, we consider the following two cases to approximate β^* in (4).

- *Case 1:* If for any $i \in [K]$, $n_i = N/K$, and $\sum_{i,j=1,i<j}^{K} \tilde{M}_{i,j} \ll \sum_{i=1}^{K} \tilde{M}_i$, then (4) is simplified to $\beta^* = 1$. In Example 4, since $\tilde{M}_i = \|A_i B_i\|_F^2$ and $\tilde{M}_{i,j} = \text{Tr}\left((A_i B_i)^T (A_j B_j)\right)$, condition $\sum_{i,j=1,i<j}^{K} \tilde{M}_{i,j} \ll \sum_{i=1}^{K} \tilde{M}_i$ holds (in expectation) if the entries of A_i and B_i are i.i.d and have zero mean and high variance.

- *Case 2:* If for any $i \in [K]$, $n_i = N/K$, and $\sum_{i,j=1,i<j}^{K} \tilde{M}_{i,j} \gg \sum_i \tilde{M}_{i=1}^{K}$, then (4) is simplified to

$$\beta^* \approx \frac{\gamma_i + \gamma_j}{2\gamma_{i,j}} = \frac{\left(\binom{N}{m} - 2\binom{N-N/K}{m} + \binom{N-2N/K}{m}\right)}{\left(\binom{N}{m} - \binom{N-N/K}{m}\right)}. \tag{5}$$

In Example 4, the condition $\sum_{i,j=1,i<j}^{K} \tilde{M}_{i,j} \gg \sum_{i=1}^{K} \tilde{M}_i$ can be obtained (in expectation) when the entries of A_i and B_i are independent and have mean zero, and A_i (and B_i) are strongly and positively correlated. Two matrices A_i and A_j are said to be correlated if any (e,k)th entries in A_i and A_j, i.e., $(A_i)_{e,k}$ and $(A_j)_{e,k}$, are correlated.

V. SIMULATION RESULTS

In this section, we experimentally compare our SAC methods and benchmark them against the state-of-the-art ϵ-approximate MatDot codes [20]. We conduct experiments in Python using double-precision floating-point numbers with machine epsilon approximately equal to 2.22×10^{-16}. We simulate the task of computing a matrix product when the task is distributed across $N = 24$ workers. Throughout this section, the task is to multiply a 100×8000 matrix A with an 8000×100 matrix B. Unless otherwise specified, the entries of A and B are real numbers selected independently from zero-mean and unit variance normal distributions. We next detail how we simulate the distributed implementation of the matrix product.

In each experiment, we first implement the encoder of the different CDC schemes. For each CDC scheme, we generate N pairs of evaluated encoding polynomials and multiply them to produce N different evaluations of the decoding polynomial. We then *uniformly* shuffle these N evaluated decoding polynomials, where the mth element will correspond to the decoding polynomial computed by the mth fastest worker. The decoder that is implemented based on the first $m \in [N]$ evaluations outputs a matrix $\tilde{C}_m \in \mathbb{R}^{100 \times 100}$, an estimate of AB. For each coding scheme, we report the relative error between AB and $\tilde{C}_m$ starting with the first $m \in [N]$ such that the scheme can provide an estimate. Due to the randomness in the permutation of (A_i, B_i) pairs and the randomness in the order of workers' completion, we repeat each experiment 100 times and report average relative errors.

In Sec. V-A, we characterize two sources of error, approximation and computation errors, both of which affect the relative error. We provide numerical experiments that compare group-wise and layer-wise SAC in terms of these sources of error. To benchmark our SAC methods against ϵ-approximate MatDot codes, in Sec. V-B, we numerically explore the tradeoff between relative error and approximation threshold. Based on Theorems 1 and 2, we optimally set the parameters of SAC showing that SAC outperforms ϵ-approximate MatDot codes in at least two ways. First, SAC lowers the approximation threshold of ϵ-approximate MatDot codes. Second, SAC reduces the relative error given the same approximation threshold used by ϵ-approximate MatDot codes.

A. Sources of Errors

We now consider two distinct sources of error: approximation and computation. Approximation error refers to the difference between the original AB product and its *best* approximation that can be derived analytically when only a subset of workers complete their tasks. Recall from Sec. III and IV that we used C_m to denote the best (analytical) approximate of $C = AB$ which can be recovered when the m fastest workers report in, and we term $\|C - C_m\|_F^2$ the approximation error. This error results from the truncation in the calculation contributed to by only a subset of workers and neglects the error caused by numerical computation and estimation. In contrast, computation error refers to the difference between the C_m and its estimate that is computed in reality. There are two major sources of computation error. One is the numerical error in the encoding and decoding computations. The other one is the error of estimating the decoding polynomial which is used for approximation recovery (e.g., the error of estimating $\hat{P}_l(x)$ by $\hat{S}_A(x)\hat{S}_B(x)$ in two-group SAC). As before, $\tilde{C}_m$ is used to denote the estimated computation of C_m. In other words, the approximate C_m is an exact version of $\tilde{C}_m$. We term $\|C_m - \tilde{C}_m\|_F^2$ the computation error.

While approximation and computation errors have been (separately) analyzed in prior work [13], [20], [22], in this paper, we introduce the notion of *total* error that accounts for both approximation and computation errors. For simplicity of notation, we denote the total error by *error* in this paper. Applying the triangle inequality to the Frobenius norm, we can bound the total error in terms of the approximation and computation errors as

$$\sqrt{\underbrace{\|C - \tilde{C}_m\|_F^2}_{\text{Error}}} \leq \sqrt{\underbrace{\|C - C_m\|_F^2}_{\text{Approximation error}}} + \sqrt{\underbrace{\|C_m - \tilde{C}_m\|_F^2}_{\text{Computation error}}} \quad (6)$$

In the sequel, we define the *relative* error, where we normalize each error by $\|C\|_F^2$. Note that Figs 2(a)-(d) are dual y-axis plots. The left y-axis corresponds to the average relative approximation error and corresponds to the black solid curves. The right y-axis corresponds to the average relative computation error and corresponds to the red dashed or dotted curves. In Figs. 2a and 2b, we plot these two quantities versus the number of completed tasks for group-wise and layer-wise SAC. We use a group-wise SAC (G-SAC) that consists of

$G = 3$ groups. As in Example 2, we set $K = 8$, and for each group we respectively set $K_1 = 2, K_2 = 4$, and $K_3 = 2$. In G-SAC, we consider two different choices of evaluation points. First, we select evaluation points to be equidistant on the real line, in particular the set $\mathcal{X}_{\text{equal}} = \{\frac{\epsilon n}{N}\}_{n=1}^N$, where $N = 24$ and ϵ is small. In Fig. 2a, we fix ϵ to be equal to 0.45, and in Fig. 2c we present results for a variety of choices for ϵ, $\epsilon \in \{10^{-3}, 3\times10^{-3}, 6\times10^{-3}, 10^{-2}, 3\times10^{-2}, 6\times10^{-2}, 10^{-1}\}$. Second, we select the N evaluation points to be complex and at equal-magnitude, $\mathcal{X}_{\text{complex}} = \{\epsilon e^{i2\pi n/24}\}_{n=1}^{24}$, where ϵ equals 0.15 in Fig. 2a and varies, $\epsilon \in \{10^{-3}, 3 \times 10^{-3}, 6 \times 10^{-3}, 10^{-2}, 3 \times 10^{-2}, 6 \times 10^{-2}, 10^{-1}\}$ in Fig. 2c. The red dashed curves plot results for $\mathcal{X}_{\text{G-SAC}} = \mathcal{X}_{\text{equal}}$, and the red dotted curves for $\mathcal{X}_{\text{G-SAC}} = \mathcal{X}_{\text{complex}}$. For layer-wise SAC (L-SAC), we use OrthoMatDot codes [13] using a similar setting to Example 3. We use $K = 8$ for a fair comparison and the evaluation set equals $\mathcal{X}_{\text{L-SAC}} = \{z_{k,i}\}_{k\in[8], i\in[3]}$, where the $z_{k,i}$ are ϵ-close to $\eta_i^{(8)}$ (the roots of $O_8(x)$). In Fig. 2b, we fix ϵ to be equal to 0.0125, and in Fig. 2d we vary $\epsilon \in \{10^{-5}, 3 \times 10^{-5}, 6 \times 10^{-5}, 10^{-4}\}$.

Considering the black solid curves in Figs. 2a and 2b, we observe that the average relative approximation error is non-increasing in the number of workers (m) that have completed their tasks. This meets our expectations and can be explained via the concept of underfitting. When m is small, a smaller number of workers have completed their tasks and thus a decoder of lower complexity tends to underfit the computations that have been completed thus far. For example, in the case of polynomial interpolation, a lower degree polynomial needs to be interpolated when m is small. As m increases, more workers complete their tasks and a more complex decoder must be used to recover the desired AB product. This monotonically non-increasing change in relative approximation error experiences three distinct drops in error in Fig. 2a. These drops occur when groups of layers complete, i.e., when m equals $R_{\text{G-SAC},1} = 2, R_{\text{G-SAC},7} = 8$, or $R_{\text{G-SAC},17} = 18$. At these values of m, the estimate $\tilde{C}_m$ is formed by adding $\sum_{j=1}^2 A_{i_j} B_{i_j}, \sum_{j=3}^6 A_{i_j} B_{i_j}$, and $\sum_{j=7}^8 A_{i_j} B_{i_j}$. On the other hand, Fig. 2b indicates a smooth decrease of the average relative approximation error for L-SAC as m increases. At $m = 15$, exact recovery is possible and an average relative approximation error of zero is obtained.

The change in error as m increases, while being monotonically non-increasing for relative approximation error, is not monotonic for relative computation error. In Fig. 2a, as the red dashed and dotted lines show, the relative computation errors increase at specific values of $m \in \{2, 8, 18\}$ and decrease in m for other values. To derive an explanation we must consider two opposing trends. On the one hand, we note that an increase in m makes the decoding procedure more complex. More complex decoding is more subject to numerical instability [13]. A larger computation error is the result. On the other hand, as m increases, the decoder used by approximate recovery estimates the decoder of exact recovery more precisely. Therefore, the estimated computation $\tilde{C}_m$ should converge to C_m as m increases, lowering the average relative computation error.

(a) G-SAC, $\epsilon = 0.45$ for $\mathcal{X}_{\text{equal}}$, $\epsilon = 0.15$ for $\mathcal{X}_{\text{complex}}$

(b) L-SAC, $\epsilon = 0.0125$ for $\mathcal{X}_{\text{L-SAC}}$

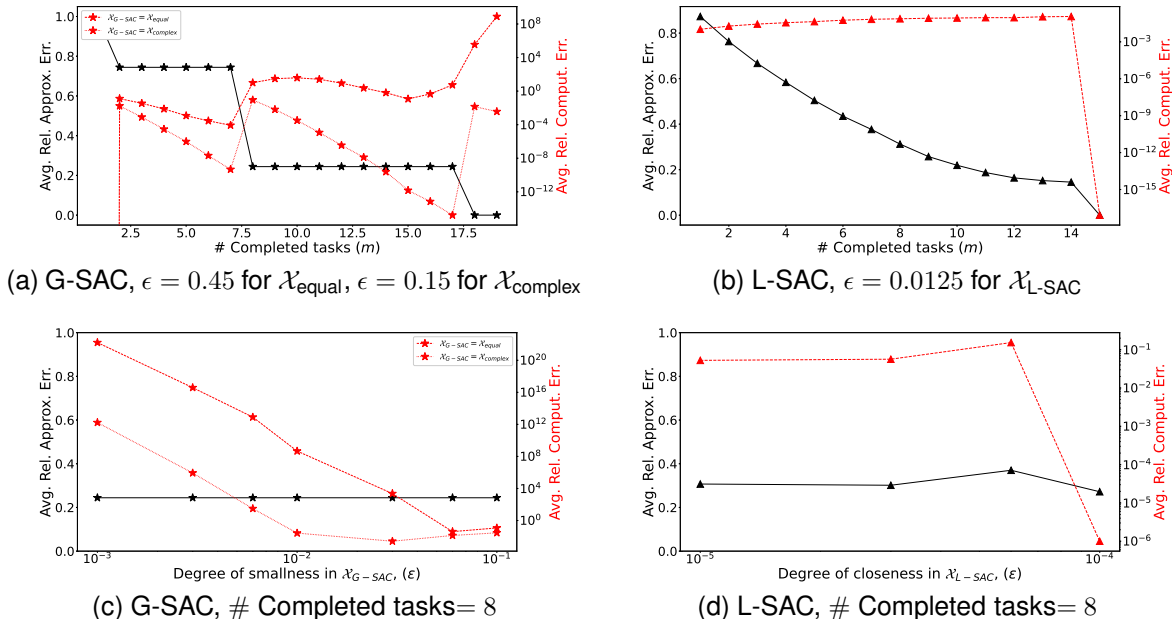(c) G-SAC, # Completed tasks$= 8$

(d) L-SAC, # Completed tasks$= 8$

Fig. 2. A dual y-axis (average relative approximation error, average relative computation error) vs. number of completed tasks in (a,b); vs. ϵ of $\mathcal{X}_{\text{G-SAC}}$ in (c); and vs. ϵ of $\mathcal{X}_{\text{L-SAC}}$ in (d). In (a,b), $\epsilon = 0.45$ if $\mathcal{X}_{\text{G-SAC}} = \mathcal{X}_{\text{equal}}$, and $\epsilon = 0.15$ if $\mathcal{X}_{\text{G-SAC}} = \mathcal{X}_{\text{complex}}$. In (c,d), number of workers is equal to 8.

We now consider these two opposing trends as m increases. In Fig. 2a, the average relative approximation error of G-SAC increases only when $m \in \{2, 8, 18\}$. At these values of m, an additional coefficient of the decoding polynomial (corresponding to $\sum_{j=1}^{2} A_{i_j} B_{i_j}$, $\sum_{j=3}^{6} A_{i_j} B_{i_j}$, or $\sum_{j=7}^{8} A_{i_j} B_{i_j}$) contributes to the AB recovery. When a new coefficient of a decoding polynomial is added to $\tilde{C}_m$, numerical stability issues that affect the computation error become more significant. But, when m increases for other values ($m \neq 2, 8$, or 18), then $\tilde{C}_m$ gets close to C and we observe a decrease in average relative computation error. In Fig. 2b, the red dashed line shows that the average relative computation error of L-SAC increases slightly as m increases up to $m = 15$. This is because $m = \sum_{k=1}^{K} m_k$ and as m increases from 1 to 14, the more likely m_k random variables become non-zero. Recalling the definitions of $\tilde{C}_m$ and C_m from (2) and (3), $m_k \neq 0$ for more indices $k \in [8]$ means that more non-zero terms are added to form both $\tilde{C}_m$ and C_m. The terms that are newly added to $\tilde{C}_m$ differ from those added to C_m. This increases the average relative computation error. However, when $m = 15$, L-SAC can recover C almost exactly, and thus a negligible average relative computation error ($\approx 10^{-17}$) is observed.

One factor that affects the relative computation error is the choice of evaluation sets, $\mathcal{X}_{\text{G-SAC}}$ and $\mathcal{X}_{\text{L-SAC}}$. Figures 2a and 2c show that the choice $\mathcal{X}_{\text{G-SAC}} = \mathcal{X}_{\text{complex}}$ outperforms the choice $\mathcal{X}_{\text{G-SAC}} = \mathcal{X}_{\text{equal}}$, as the former (the red dotted curves) have a lower average relative computation error than the latter (the red dashed curves). We can understand this as resulting from the condition number of the Vandermonde matrix in the G-SAC decoder. When evaluation points are selected from $\mathcal{X}_{\text{equal}}$, the G-SAC decoder solves a system of linear equations that involves a real Vandermonde matrix. However, when sampling using $\mathcal{X}_{\text{complex}}$, the entries of the Vandermonde matrix

are complex entries of equal magnitude, i.e., located on a circle in $\mathbb{C}$. As is shown in [22], the condition number of a real Vandermonde matrix exponentially grows in m, while when the entries are chosen from $\mathcal{X}_{\text{complex}}$ the condition number of the Vandermonde matrix grows only polynomially in m. Ill-conditioning leads to numerical problems which contribute to the relative computation error. This explains the superiority of $\mathcal{X}_{\text{complex}}$ over $\mathcal{X}_{\text{equal}}$ in terms of relative computation error. That said, since each complex multiplication is equivalent to four real multiplications, the use of complex evaluation points from $\mathcal{X}_{\text{complex}}$ increases the computation load of each worker by a factor of four when compared to the use of real evaluation points in $\mathcal{X}_{\text{equal}}$. Thus, despite lower relative computation error, a downside to the use of $\mathcal{X}_{\text{complex}}$ is the increased computation.

Another way to lower the relative computation error of G-SAC is to set its evaluation points to be sufficiently small. In Fig. 2c, we fix $m = 8$ and show that the average relative computation error of G-SAC is minimized by setting $\epsilon = 3 \times 10^{-2}$ in $\mathcal{X}_{\text{complex}}$ and to $\epsilon = 6 \times 10^{-2}$ in $\mathcal{X}_{\text{equal}}$. Similarly, in Fig. 2d, we show that the average relative computation error of L-SAC is minimized by setting $\epsilon = 10^{-4}$ in $\mathcal{X}_{\text{L-SAC}}$. We now make two comments. First, note that as both Figs. 2c and 2d indicate, setting ϵ lower than some threshold increases the average relative computation error. This is due to the finite precision of simulations. Second, in contrast to computation error, the relative approximation error is independent of ϵ. The black solid curves in Figs. 2c and 2d show that the average relative approximation errors of both G-SAC and L-SAC are approximately equal to 0.3 when we fix $m = 8$ and vary ϵ.

B. Fundamental Tradeoffs

In contrast to the previous section, where we evaluated relative approximation error and relative computation error

separately, in this section we jointly consider these two sources of error. We label curves for two group-wise SAC (G-SAC), for two layer-wise SAC (L-SAC), and for ϵ-approximate MatDot codes [20] using, respectively, star, triangular, and square marks. To ensure a fair comparison, we set $K = 8$ for all curves. For the G-SAC implementations, we use two-group SAC twice, one with $K_1 = 5$ and the other with $K_1 = 8$. In both, we select N evaluation points from $\mathcal{X}_{\text{complex}} = \{0.1 e^{i2\pi n/N}\}_{n=1}^N$, where $N = 24$. For the two L-SAC implementations, we use OrthoMatDot [13] and Lagrange [11] codes with settings similar to those used in Examples 3 and 4. In particular, for OrthoMatDot L-SAC, the evaluation set $\mathcal{X}_{\text{L-SAC}}$ equals $\{z_{k,i}\}_{k\in[8], i\in[3]}$, where the $z_{k,i}$ are ϵ-close to η_k^8 and $\epsilon = 6.25 \times 10^{-3}$. For Lagrange L-SAC, $\mathcal{X}_{\text{L-SAC}}$ equals $\{y_{k,i}\}_{k\in[8], i\in[3]}$, where the $y_{k,i}$ are ϵ-close to y_k, $\epsilon = 3.33 \times 10^{-2}$, and $y_k = k$ for any $k \in [8]$.

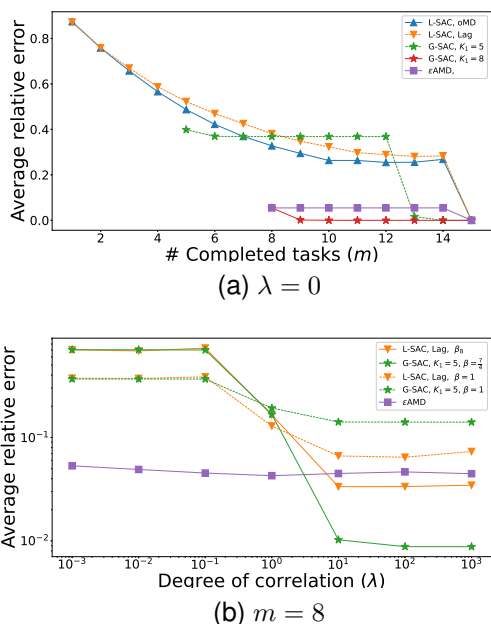(a) $\lambda = 0$

(b) $m = 8$

Fig. 3. Average relative error vs. (a) the number of completed tasks (m), where $\lambda = 0$; vs. (b) the degree of correlation (λ), where $m = 8$.

Relative error vs. approximation threshold: We first plot average relative error vs. the number of completed tasks (m) in Fig. 3a. Note that the m that varies from 1 to 14 is a variable representing the approximation threshold. The $m = 15$ is the recovery threshold. Figure 3a shows that while all CDC schemes are able to recover AB with (almost) zero error when $m = 15$, they achieve different tradeoffs between average relative error and approximation threshold (when $m < 15$). As Fig. 3a shows the ϵ-approximate MatDot code provides an estimate of AB, only once when $m = 8$. It then needs to wait for exact recovery (until $m = 15$) to improve on this estimate. However, the other four SAC methods can improve on this tradeoff even when $m < 15$.

The G-SAC method (the red solid curve) must wait until $m = 8$ to provide its first estimate; This is similar to ϵ-approximate MatDot codes. However, in contrast to ϵ-approximate MatDot codes, the G-SAC method improves on this estimate as m increases by achieving a close to zero av-

erage relative error before exact recovery. The G-SAC method (the green dashed curve) can provide an earlier estimate (when $m = 5$) compared to the previous two methods. It then gradually improves on this estimate when m increases up to $m = 13$. However, when $m < 13$, the estimate that this G-SAC method provides has a higher average relative error, compared to the previous two methods. When $m = 13$, the average relative error of the second G-SAC method displays a significant drop such that it outperforms ϵ-approximate MatDot codes. Indeed, this G-SAC method can achieve an average relative error close to zero when $m = 14$; similar to the first G-SAC method.

The two L-SAC methods are able to produce estimates of AB since $m = 1$, and continuously improve on average relative error as m increases above 1. However, as shown in Fig. 3a, only when $7 \leq m < 13$ can the OrthoMatDot L-SAC method provide a lower average relative error than can the second G-SAC method. This range of m is even smaller for the Lagrange L-SAC method. This method only outperforms the second G-SAC method in terms of average relative error when $9 \leq m < 13$. Figure 3a shows that despite providing earlier estimates, L-SAC methods do not achieve lower average relative error when compared to the first G-SAC and ϵ-approximate MatDot codes. That said, we next describe situations in which Lagrange L-SAC methods can achieve lower average relative error than ϵ-approximate MatDot code even when $m \geq 8$.

Effect of correlation: We note that in all previous figure, the entries of A and B are assumed to be independently selected from the zero-mean and unit variance normal distribution. This populates A and B matrices with both positive and negative entries, and the $A_i B_i$ matrices are uncorrelated for all $i \in [8]$. With respect to Remark 4, we define two matrices $A_i B_i$ and $A_j B_j$ to be uncorrelated if

$$\text{Tr}\left(\mathbb{E}\left((A_i B_i)^T (A_j B_j)\right)\right) = \text{Tr}\left(\mathbb{E}\left(A_i B_i\right)^T \mathbb{E}\left(A_j B_j\right)\right) \quad (7)$$

and to be correlated otherwise. This condition is obtained directly from the assumption that any $(A_i B_i)_{e,k}$ and $(A_j B_j)_{e,k}$ entries in $A_i B_i$ and $A_j B_j$ are uncorrelated. In other words, (7) is obtained based on the assumption that $\mathbb{E}((A_i B_i)_{e,k}(A_j B_j)_{e,k}) = \mathbb{E}((A_i B_i)_{e,k})\mathbb{E}((A_j B_j)_{e,k})$. We next consider a situation where $\{A_i B_i\}$ are correlated. We construct the A_i and B_i matrices as $A_i = \lambda A^{(0)} + A_i^{(1)}$ and $B_i = \lambda B^{(0)} + B_i^{(1)}$, where λ is the degree of correlation. In this construction, $A^{(0)}$ and $B^{(0)}$ are latent random matrices common to all the A_i and B_i. The $A_i^{(1)}$ and $B_i^{(1)}$ are random matrices that are specific to the ith matrices A_i and B_i. As before, the entries of the $A^{(0)}$, $A_i^{(1)}$, $B^{(0)}$, and $B_i^{(1)}$ matrices are selected independently from the zero-mean and unit-variance normal distribution for all $i \in [8]$. The correlation degree λ plays a key role. The correlation between $A_i B_i$ and $A_j B_j$ when $i \neq j$ is

$$\mathbb{E}\left(\text{Tr}\left((A_i B_i)^T (A_j B_j)\right)\right) = \lambda^4 \mathbb{E}\left(\|A^{(0)} B^{(0)}\|_F^2\right), \quad (8)$$

while when $i = j$ is

$$\mathbb{E}\left(\mathrm{Tr}\left((A_i B_i)^T (A_i B_i)\right)\right) = \mathbb{E}\left(\|A_i B_i\|_F^2\right)$$
$$= \lambda^4 \mathbb{E}\left(\|A^{(0)} B^{(0)}\|_F^2\right) + \lambda^2 \mathbb{E}\left(\|A^{(0)} B_i^{(1)}\|_F^2\right) +$$
$$+ \lambda^2 \mathbb{E}\left(\|A_i^{(1)} B^{(0)}\|_F^2\right) + \mathbb{E}\left(\|A_i^{(1)} B_i^{(1)}\|_F^2\right). \quad (9)$$

We now consider two cases. First, when λ is close to zero. In this case, (8) is almost zero while (9) equals $\mathbb{E}\left(\|A_i^{(1)} B_i^{(1)}\|_F^2\right)$, which is nonzero. Second, when $\lambda \gg 1$, both (8) and (9) are almost equal to $\lambda^4 \mathbb{E}\left(\|A^{(0)} B^{(0)}\|_F^2\right)$. These two cases can be viewed in analogy with the two cases considered in Remark 4 and Example 4. Accordingly, when $\lambda \approx 0$, the approximation error of G-SAC can be minimized if we set $\beta = 1$ in (1). Similarly, the L-SAC method that applies to Lagrange codes achieves the minimum approximation error if β in (4) is set to 1. When $\lambda \gg 1$, we can set $\beta = \frac{7}{4}$ in (1) to minimize the approximation error of G-SAC. We can also set β according to (5) for L-SAC. Note that since β in (5) is a function of m, we represent it with an additional subscript m, β_m, in the remainder of this section.

In Fig. 3b, we plot average relative error vs. λ, where $\lambda \in \{10^{-3}, 10^{-2}, 10^{-1}, 1, 10, 10^2, 10^3\}$ and $m = 8$. The results for L-SAC when used with Lagrange codes and β_8 is plotted by the orange solid curve; when $\beta = 1$, the result is plotted by the orange dashed curve. Similarly, we plot (green solid curve) the result for G-SAC when $\beta = \frac{7}{4}$ and plot (green dashed curve) the results for $\beta = 1$. In both G-SAC methods, we fix $K_1 = 5$. As shown in Fig. 3b, when $\lambda \leq 1$, we can lower the average relative error of the G-SAC and L-SAC methods by setting $\beta = 1$. In this case, while the ϵ-approximate MatDot codes provide its first estimate, the average relative error of this estimate is lower than those of the G-SAC with $K_1 = 8$ and L-SAC. A similar effect is also seen in Fig. 3a for $m = 8$, where we used uncorrelated input matrices ($\lambda = 0$). On the other hand, Figure 3b shows that when $\lambda \geq 10$, both G-SAC and L-SAC provide lower average relative errors compared to ϵ-approximate MatDot codes if their β are respectively set to $\frac{7}{4}$ and β_8.

VI. CONCLUSION

In this paper, we propose group-wise and layer-wise SAC which enable approximate computing in prior CDC schemes. Our SAC schemes extend the approximation procedure into multiple resolution layers beyond the single layer of ϵ-approximate MatDot codes [20]. We analytically and experimentally studied different sources of error in SAC and provided design guidelines. Our simulations justify the superiority of SAC over ϵ-approximate MatDot codes [20] by achieving a better tradeoff between approximation threshold and relative error. Optimally setting parameters in SAC not only provides a lower approximation threshold but also yields a lower relative error when compared to ϵ-approximate MatDot codes.

While our paper focuses on matrix multiplication where polynomial-based CDC is applied, a direct extension of this paper is to apply SAC to more practical applications such as training deep neural networks. Another extension is to use SAC in a distributed system composed of a heterogeneous set of workers of different computational abilities. We aim to provide optimal parameters of SAC with respect to such a heterogeneous distributed system in future works.

REFERENCES

[1] K. Lee, M. Lam, R. Pedarsani, D. Papailiopoulos, and K. Ramchandran, "Speeding up distributed machine learning using codes," *IEEE Trans. Inf. Theory*, vol. 64, no. 3, pp. 1514–1529, 2017.
[2] S. Dutta, V. Cadambe, and P. Grover, "Short-dot: Computing large linear transforms distributedly using coded short dot products," *Int. Conf. Neural Inf. Proc. Sys. (NeurIPS)*, vol. 29, 2016.
[3] K. Lee, C. Suh, and K. Ramchandran, "High-dimensional coded matrix multiplication," in *IEEE Int. Symp. Inf. Theory (ISIT)*, 2017, pp. 2418–2422.
[4] Q. Yu, M. A. Maddah-Ali, and A. S. Avestimehr, "Polynomial codes: an optimal design for high-dimensional coded matrix multiplication," in *Int. Conf. Neural Inf. Proc. Sys. (NeurIPS)*, 2017, pp. 4406–4416.
[5] S. Dutta, M. Fahim, F. Haddadpour, H. Jeong, V. Cadambe, and P. Grover, "On the optimal recovery threshold of coded matrix multiplication," *IEEE Trans. on Inf. Theory*, vol. 66, no. 1, pp. 278–301, 2019.
[6] S. Kiani, N. Ferdinand, and S. C. Draper, "Exploitation of stragglers in coded computation," in *IEEE Int. Symp. Inf. Theory (ISIT)*, 2018, pp. 1988–1992.
[7] ——, "Hierarchical coded matrix multiplication," *IEEE Trans. Inf. Theory*, vol. 67, no. 2, pp. 726–754, 2020.
[8] A. Mallick, M. Chaudhari, U. Sheth, G. Palanikumar, and G. Joshi, "Rateless codes for near-perfect load balancing in distributed matrix-vector multiplication," *Proc. of the ACM on Measurement and Analysis of Computing Sys*, vol. 3, no. 3, pp. 1–40, 2019.
[9] Q. Yu, M. A. Maddah-Ali, and A. S. Avestimehr, "Straggler mitigation in distributed matrix multiplication: Fundamental limits and optimal coding," *IEEE Trans. Inf. Theory*, vol. 66, no. 3, pp. 1920–1933, 2020.
[10] S. Dutta, Z. Bai, H. Jeong, T. M. Low, and P. Grover, "A unified coded deep neural network training strategy based on generalized polydot codes," in *IEEE Int. Symp. Inf. Theory (ISIT)*. IEEE, 2018, pp. 1585–1589.
[11] Q. Yu, S. Li, N. Raviv, S. M. M. Kalan, M. Soltanolkotabi, and S. A. Avestimehr, "Lagrange coded computing: Optimal design for resiliency, security, and privacy," in *Int. Conf. on Artificial Intelligence and Statistics (AISTATS)*, 2019, pp. 1215–1225.
[12] A. Quarteroni, R. Sacco, and F. Saleri, *Numerical mathematics*. Springer Science & Business Media, 2010, vol. 37.
[13] M. Fahim and V. R. Cadambe, "Numerically stable polynomially coded computing," *IEEE Trans. on Inf. Theory*, vol. 67, no. 5, pp. 2758–2785, 2021.
[14] N. Charalambides, M. Pilanci, and A. O. Hero, "Approximate weighted cr coded matrix multiplication," in *IEEE Int. Conf. Acoustics, Speech and Signal Processing (ICASSP)*, 2021, pp. 5095–5099.
[15] W.-T. Chang and R. Tandon, "Random sampling for distributed coded matrix multiplication," in *IEEE Int. Conf. Acoustics, Speech and Signal Processing (ICASSP)*, 2019, pp. 8187–8191.
[16] N. S. Ferdinand and S. C. Draper, "Anytime coding for distributed computation," in *IEEE Annual Allerton Conf. on Commun., Control, and Comput.*, 2016, pp. 954–960.
[17] J. Zhu, Y. Pu, V. Gupta, C. Tomlin, and K. Ramchandran, "A sequential approximation framework for coded distributed optimization," in *IEEE Annual Allerton Conf. on Commun., Control, and Comput.*, 2017, pp. 1240–1247.
[18] T. Jahani-Nezhad and M. A. Maddah-Ali, "Codedsketch: A coding scheme for distributed computation of approximated matrix multiplication," *IEEE Trans. Inf. Theory*, vol. 67, no. 6, pp. 4185–4196, 2021.
[19] V. Gupta, S. Wang, T. Courtade, and K. Ramchandran, "Oversketch: Approximate matrix multiplication for the cloud," in *IEEE Int. Conf. on Big Data*, 2018, pp. 298–304.
[20] H. Jeong, A. Devulapalli, V. R. Cadambe, and F. P. Calmon, "ϵ−approximate coded matrix multiplication is nearly twice as efficient as exact multiplication," *IEEE J. Sel. Areas Inf. Theory*, vol. 2, no. 3, pp. 845–854, 2021.
[21] P. Drineas, R. Kannan, and M. W. Mahoney, "Fast Monte Carlo algorithms for matrices I: Approximating matrix multiplication," *SIAM J. on Comput.*, vol. 36, no. 1, pp. 132–157, 2006.
[22] A. Ramamoorthy and L. Tang, "Numerically stable coded matrix computations via circulant and rotation matrix embeddings," in *IEEE Int. Symp. Inf. Theory (ISIT)*, 2021, pp. 1712–1717.

APPENDIX

A. Admissible Ranges for Number of Resolution Layers

In this section, we prove the maximum and minimum admissible bounds on the number of resolution layers in group-wise SAC.

Claim 1: In group-wise SAC, the number of layers is in the ranges $R_{\text{G-SAC}} - K \leq L_{\text{S}\epsilon\text{AMD}} \leq R_{\text{G-SAC}} - 1$.

Proof: Since the exact recovery is achieved at $R_{\text{G-SAC}}$ and the approximation threshold increases as $R_{\text{G-SAC},l} = R_{\text{G-SAC},l-1} + 1$ for each $l \in \{2, 3, \ldots L_{\text{G-SAC}}\}$, the following formula holds for the last resolution layer. We have $R_{\text{G-SAC},L_{\text{G-SAC}}} = R_{\text{G-SAC},1} + L_{\text{G-SAC}} - 1$ which equals to $R_{\text{G-SAC}} - 1$. Therefore, $L_{\text{G-SAC}} = R_{\text{G-SAC}} - R_{\text{G-SAC},1}$. Since $R_{\text{G-SAC},1} \in [K]$, we can conclude that $L_{\text{G-SAC}} \in \{R_{\text{G-SAC}} - K, \ldots, R_{\text{G-SAC}} - 1\}$. ∎

B. Proof of Thm. 1

Recalling the notation from Sec. III, in resolution layer $l \in [L_{\text{G-SAC}}]$ of group-wise SAC, the master recovers $C_l = \sum_{k=1}^{m_l} A_{i_k} B_{i_k}$ to some accuracy. Also, assume that the $A_{i_1} B_{i_1}, \ldots, A_{i_K} B_{i_K}$ products are a *uniform* random permutation of $A_1 B_1, \ldots, A_K B_K$. We first calculate the expected value of C_l, proving that the scaled sum $\frac{K}{m_l} C_l$ is an unbiased estimate of $C = AB$. We compute $\mathbb{E}\left(\frac{K}{m_l} \sum_{k=1}^{m_l} A_{I_k} B_{I_k}\right)$, where the expectation is taken with respect to the random indices $\{I_k\}_{k=1}^K$.

$$\mathbb{E}\left(\frac{K}{m_l} \sum_{k=1}^{m_l} A_{I_k} B_{I_k}\right)$$

$$\stackrel{(1)}{=} \frac{K}{m_l} \sum_{i_1,\ldots,i_K} \left(\left(\sum_{k=1}^{m_l} A_{i_k} B_{i_k}\right) P(I_1 = i_1, \ldots, I_K = i_K)\right)$$

$$\stackrel{(2)}{=} \frac{K}{m_l} \sum_{j=1}^K A_j B_j P(j \in \{I_k\}_{k=1}^{m_l})$$

$$\stackrel{(3)}{=} \frac{K}{m_l} \sum_{j=1}^K A_j B_j \left(1 - P\left(j \in \{I_k\}_{k=m_l+1}^K\right)\right)$$

$$\stackrel{(4)}{=} \frac{K}{m_l} \sum_{j=1}^K A_j B_j \left(1 - \frac{\binom{K-1}{m_l}}{\binom{K}{m_l}}\right)$$

$$\stackrel{(5)}{=} \frac{K}{m_l} \sum_{j=1}^K A_j B_j \frac{m_l}{K} = \sum_{j=1}^K A_j B_j = AB. \qquad (10)$$

In (10), the first equality is obtained by expanding the expected value as the weighted sum of the $\frac{K}{m_l} \sum_{k=1}^{m_l} A_{i_k} B_{i_k}$ values, with the probabilities $P(I_1 = i_1, \ldots, I_K = i_K)$ as the weights. In this expansion, the sample $(i_1, \ldots, i_k)$ is the realization of K random variables $(I_1, \ldots, I_K)$, whose values depend on the indices of the random permutation of $A_1 B_1, \ldots, A_K B_K$. The second equality of (10) is a result of rewriting $\sum_{i_1,\ldots,i_K, j \in \{i_k\}_{k=1}^{m_l}} P(I_1 = i_1, \ldots, I_K = i_K)$ by $P(j \in \{I_k\}_{k=1}^{m_l})$. In the third equality of (10), the probability of the event $j \in \{I_k\}_{k=1}^{m_l}$ occurs is replaced with 1 minus the probability of the event does not occur. In the forth equality of (10), $\binom{K}{m_l}$ is the total number of ways that m_l

(distinct) indices are picked first from $\{1, \ldots, K\}$. If index j is excluded, then there are $K - 1$ other indices and $\binom{K-1}{m_l}$ ways to choose the first m_l indices from $\{1, \ldots, K\}/\{j\}$. In the last equations, we simplify the expressions and prove that $\mathbb{E}\left(\frac{K}{m_l} \sum_{k=1}^{m_l} A_{I_k} B_{I_k}\right)$ equals AB in (10).

We next solve for the scaling β that is the solution to $\text{argmin}_\beta \mathbb{E}\left(\|C - \beta C_l\|_F^2\right)$. Since the problem is convex is β, we set the derivative to zero and find β^*. We start by expanding $\mathbb{E}\left(\|C - \beta C_l\|_F^2\right)$ as

$$\|C\|_F^2 - 2\beta \text{Tr}\left(C^T \mathbb{E}(C_l)\right) + \beta^2 \mathbb{E}\left(\|C_l\|_F^2\right)$$

$$\stackrel{(1)}{=} \|C\|_F^2 \left(1 - 2\beta \frac{m_l}{K}\right) + \beta^2 \mathbb{E}\left(\|C_l\|_F^2\right)$$

$$\stackrel{(2)}{=} \|C\|_F^2 \left(1 - 2\beta \frac{m_l}{K}\right) + \beta^2 \left(\sum_{j=1}^K \left(\|A_j B_j\|_F^2 P(j \in \{i_k\}_{k=1}^{m_l})\right)\right.$$

$$\left. + 2 \sum_{\substack{j,j'=1 \\ j'<j}}^K \left(\text{Tr}\left((A_{j'} B_{j'})^T (A_j B_j)\right) P(j, j' \in \{i_k\}_{k=1}^{m_l})\right)\right)$$

$$\stackrel{(3)}{=} \|C\|_F^2 \left(1 - 2\beta \frac{m_l}{K}\right) + \beta^2 \left(\sum_{j=1}^K \left(\|A_j B_j\|_F^2 \frac{\binom{K}{m_l} - \binom{K-1}{m_l}}{\binom{K}{m_l}}\right)\right.$$

$$\left. + 2 \sum_{\substack{j,j'=1 \\ j'<j}}^K \left(\text{Tr}\left((A_{j'} B_{j'})^T (A_j B_j)\right) \frac{\binom{K}{m_l} - 2\binom{K-1}{m_l} + \binom{K-2}{m_l}}{\binom{K}{m_l}}\right)\right)$$

$$\stackrel{(4)}{=} \|C\|_F^2 \left(1 - 2\beta \frac{m_l}{K}\right) + \beta^2 \left(M_1 \frac{m_l}{K} + 2M_2 \frac{m_l(m_l - 1)}{K(K - 1)}\right), \qquad (11)$$

where

$$M_1 = \sum_{j=1}^K \|A_j B_j\|_F^2, \text{ and}$$

$$M_2 = \sum_{j,j'=1, j'<j}^K \text{Tr}\left((A_{j'} B_{j'})^T (A_j B_j)\right).$$

In the first equation of (11), we use (10) to replace $\mathbb{E}(C_l)$ with $\frac{m_l}{K} C$. The second equation is obtained by expanding $\mathbb{E}(\|C_l\|_F^2)$. To do this expansion, we use the results of second equation in (10). Similar to the logic we used in the third and forth equations of (10), in the third equation of (11) we replace $P(j \in \{i_k\}_{k=1}^{m_l})$ with $\frac{\binom{K}{m_l} - \binom{K-1}{m_l}}{\binom{K}{m_l}}$. We also replace $P(j, j' \in \{i_k\}_{k=1}^{m_l})$ with $\frac{\binom{K}{m_l} - 2\binom{K-1}{m_l} + \binom{K-2}{m_l}}{\binom{K}{m_l}}$. The intuition behind the latter replacement is similar to the former. The probability of the event $j, j' \in \{I_k\}_{k=1}^{m_l}$ occurs is equal to 1 minus the probability of at least one of j or j' are excluded plus the probability of both indices are excluded. If j (or j') are excluded, we showed that there are $\binom{K-1}{m_l}$ ways to choose the first m_l indices from $[K]/\{j\}$ (or $[K]/\{j'\}$). If both indices j and j' are excluded, then there are $K - 2$ other indices and $\binom{K-2}{m_l}$ ways to choose the first m_l indices from $[K]/\{j, j'\}$. Combining these results together, we conclude

$P(j, j' \in \{i_k\}_{k=1}^{m_l}) = \frac{\binom{K}{m_l} - 2\binom{K-1}{m_l} + \binom{K-2}{m_l}}{\binom{K}{m_l}}$. Finally, with simplifying the mathematical expressions we obtain the fourth equation in (11).

Next, we take the derivative of $\mathbb{E}\left(\|C - \beta C_l\|_F^2\right)$ with respect to β and set the result to zero. Thus, we have

$$-2\|C\|_F^2 \frac{m_l}{K} + 2\beta^* \left(M_1 \frac{m_l}{K} + 2M_2 \frac{m_l(m_l-1)}{K(K-1)}\right) = 0$$

$$\Rightarrow \beta^* = \frac{\|C\|_F^2 \frac{m_l}{K}}{\left(M_1 \frac{m_l}{K} + 2M_2 \frac{m_l(m_l-1)}{K(K-1)}\right)}.$$

Since $\|C\|_F^2 = M_1 + 2M_2$, we have

$$\beta^* = \frac{M_1 \frac{m_l}{K} + 2M_2 \frac{m_l}{K}}{\left(M_1 \frac{m_l}{K} + 2M_2 \frac{m_l(m_l-1)}{K(K-1)}\right)} = \frac{M_1 + 2M_2}{\left(M_1 + 2M_2 \frac{(m_l-1)}{(K-1)}\right)}. \blacksquare$$

C. Proof of Thm. 2

Recalling from Sec. IV, in layer-wise SAC the master recovers $C_m = \sum_{j=1}^{K} \alpha_j \tilde{S}_A(y_j)\tilde{S}_B(y_j)\mathbb{1}_{m_j>0}$ to some accuracy when m workers report in. Recall $m = \sum_{j=1}^{K} m_j$, where m_j is the number of workers that complete the evaluation of $\tilde{S}_A(y_j)\tilde{S}_B(y_j)$ to some accuracy. We next solve $\mathrm{argmin}_\beta \mathbb{E}\left(\|C - \beta C_m\|_F^2\right)$, where the expectation is taken with respect to the random m_j. To do this, we first calculate $\mathbb{E}(C_m)$.

$$\mathbb{E}(C_m) = \sum_{j=1}^{K} \alpha_j \tilde{S}_A(y_j)\tilde{S}_B(y_j)\mathbb{E}(\mathbb{1}_{m_j>0})$$

$$= \sum_{j=1}^{K} \alpha_j \tilde{S}_A(y_j)\tilde{S}_B(y_j)\gamma_j$$

where $\gamma_j = P(m_j > 0) = 1 - \binom{N-n_j}{m}/\binom{N}{m}$. This equality holds with respect to the logic we used to prove the forth equation in (10). Using the definition of C_m, we can expand $\mathbb{E}\left(\|C - \beta C_m\|_F^2\right)$ as

$$\|C\|_F^2 - 2\beta \, \mathrm{Tr}\left(C^T \mathbb{E}(C_m)\right) + \beta^2 \mathbb{E}\left(\|C_m\|_F^2\right) = \|C\|_F^2 +$$

$$-2\beta \sum_{j=1}^{K} \left[\mathrm{Tr}\left(\left(\tilde{S}_A(y_j)\tilde{S}_B(y_j)\right)^T \left(\tilde{S}_A(y_j)\tilde{S}_B(y_j)\right)\right)\alpha_j^2 \gamma_j\right]$$

$$-2\beta \sum_{\substack{j,j'=1 \\ j'<j}}^{K} \left[\mathrm{Tr}\left(\left(\tilde{S}_A(y_{j'})\tilde{S}_B(y_{j'})\right)^T \left(\tilde{S}_A(y_j)\tilde{S}_B(y_j)\right)\right)\right.$$
$$\left. \times \alpha_{j'}\alpha_j\gamma_{j'}\right]$$

$$-2\beta \sum_{\substack{j,j'=1 \\ j'<j}}^{K} \left[\mathrm{Tr}\left(\left(\tilde{S}_A(y_{j'})\tilde{S}_B(y_{j'})\right)^T \left(\tilde{S}_A(y_j)\tilde{S}_B(y_j)\right)\right)\right.$$
$$\left. \times \alpha_{j'}\alpha_j\gamma_j\right]$$

$$+\beta^2 \sum_{j=1}^{K} \left[\mathrm{Tr}\left(\left(\tilde{S}_A(y_j)\tilde{S}_B(y_j)\right)^T \left(\tilde{S}_A(y_j)\tilde{S}_B(y_j)\right)\right)\alpha_j^2 \gamma_j\right]$$

$$+2\beta^2 \sum_{\substack{j,j'=1 \\ j'<j}}^{K} \left[\mathrm{Tr}\left(\left(\tilde{S}_A(y_{j'})\tilde{S}_B(y_{j'})\right)^T \left(\tilde{S}_A(y_j)\tilde{S}_B(y_j)\right)\right)\right.$$
$$\left. \times \alpha_{j'}\alpha_j\gamma_{j',j}\right], \tag{12}$$

where $\gamma_{j',j} = \mathbb{E}(\mathbb{1}_{m_{j'},m_j>0}) = P(m_{j'}, m_j > 0)$. Using similar logic to that of third equation in (11), we can conclude that

$$\gamma_{j',j} = \frac{\binom{N}{m} - \binom{N-n_{j'}}{m} - \binom{N-n_j}{m} + \binom{N-n_{j'}-n_j}{m}}{\binom{N}{m}}.$$

Letting $\tilde{M}_{i,j} = \alpha_i\alpha_j \, \mathrm{Tr}\left(\left(\tilde{S}_A(y_i)\tilde{S}_B(y_i)\right)^T \left(\tilde{S}_A(y_j)\tilde{S}_B(y_j)\right)\right)$ and $\tilde{M}_i = \alpha_i^2 \|\tilde{S}_A(y_i)\tilde{S}_B(y_i)\|_F^2$, we can rewrite (12) as

$$\mathbb{E}\left(\|C - \beta C_m\|_F^2\right)$$

$$= \|C\|_F^2 - 2\beta \sum_{j=1}^{K} \tilde{M}_j \gamma_j - 2\beta \sum_{\substack{j,j'=1 \\ j'<j}}^{K} \tilde{M}_{j',j}(\gamma_{j'} + \gamma_j)$$

$$+ \beta^2 \sum_{j=1}^{K} \tilde{M}_j \gamma_j + 2\beta^2 \sum_{\substack{j,j'=1 \\ j'<j}}^{K} \tilde{M}_{j',j}\gamma_{j',j}.$$

To solve $\mathrm{argmin}_\beta \mathbb{E}\left(\|C - \beta C_m\|_F^2\right)$, we take the derivative of $\mathbb{E}\left(\|C - \beta C_m\|_F^2\right)$ with respect to β and set it to 0, optimizing β via

$$-2\sum_{j=1}^{K} \tilde{M}_j \gamma_j - 2\sum_{\substack{j,j'=1 \\ j'<j}}^{K} \tilde{M}_{j,j'}(\gamma_{j'} + \gamma_j) + 2\beta^* \sum_{j=1}^{K} \tilde{M}_j \gamma_j +$$

$$+ 4\beta^* \sum_{\substack{j,j'=1 \\ j'<j}}^{K} \tilde{M}_{j',j}\gamma_{j',j} = 0$$

$$\Rightarrow \beta^* = \frac{\sum_{j=1}^{K} \tilde{M}_j \gamma_j + \sum_{\substack{j,j'=1 \\ j'<j}}^{K} \tilde{M}_{j',j}(\gamma_{j'} + \gamma_j)}{\sum_{j=1}^{K} \tilde{M}_j \gamma_j + 2\sum_{\substack{j,j'=1 \\ j'<j}}^{K} \tilde{M}_{j',j}\gamma_{j',j}}. \blacksquare$$

D. Proof to $\lim_{\epsilon \to 0} \tilde{C}_m = C_m$ in layer-wise SAC

Recall from Sec. IV that in layer-wise SAC the master can compute

$$\tilde{C}_m = \sum_{k=1}^{K} \alpha_k \frac{\sum_{i=1}^{m_k} \tilde{S}_A(z_{k,j_{k,i}})\tilde{S}_B(z_{k,j_{k,i}})}{m_k}.$$

when the m fastest workers ($m = \sum_{k=1}^{K} m_k$) finish computing the $\tilde{S}_A(z_{k,j_{k,i}})\tilde{S}_B(z_{k,j_{k,i}})$ products, $k \in [K]$ and $i \in [m_k]$. Also, recall that $z_{k,i}$ is ϵ-close to y_k, for any $k \in [K]$ and all $i \in [n_k]$. We use the following lemma to prove that $\lim_{\epsilon \to 0} \tilde{C}_m = C_m$, where $C_m = \sum_{k=1}^{K} \alpha_k \tilde{S}_A(y_k)\tilde{S}_B(y_k)\mathbb{1}_{m_k>0}$.

Lemma 1: Let y be ϵ-close to x and assume that the $n-$degree polynomial $f(x) = c_0 + c_1 x + \ldots + c_n x^n$ is evaluated at x. Both x and the coefficients c_i are bounded as $|x| \leq \lambda_1$ and $|c_i| \leq \lambda_2$. The error of approximating $f(y)$ with $f(x)$ can be bounded as

$$|f(y) - f(x)| \leq \lambda_2 \left(\frac{(\lambda_1 + \epsilon)^{n+1} - (\lambda_1 + \epsilon)}{(\lambda_1 + \epsilon) - 1} - \frac{\lambda_1^{n+1} - \lambda_1}{\lambda_1 - 1}\right).$$

Proof of Lem. 1: Using the definition of $f(x)$ and $f(y)$, we first expand the error as

$$|f(y) - f(x)| = \left| \sum_{i=1}^{n} c_i(y-x)^i \right| \tag{13}$$

Replacing $(y-x)^i$ with its expansion $(y-x)\left(\sum_{j=0}^{i-1} y^j x^{i-1-j}\right)$ and using triangular inequality, we can bound (13) as

$$|f(y) - f(x)| \leq \lambda_2 \epsilon \sum_{i=1}^{n} \sum_{j=0}^{i-1} |y|^j |x|^{i-1-j}. \tag{14}$$

Note that in the above inequality, we use the bounds for $|c_i| \leq \lambda_2$ and $|y-x| \leq \epsilon$. Using the bounds for $|x| \leq \lambda_1$ and $|y| \leq |x| + \epsilon \leq \lambda_1 + \epsilon$, we can further upper bound the right-hand-side of (14). In the following we provide this upper bound. We then in the first and second equations simplify the mathematical expressions using the close form of geometric series, and prove the lemma.

$$|f(y) - f(x)| \leq \lambda_2 \epsilon \sum_{i=1}^{n} \sum_{j=0}^{i-1} (\lambda_1 + \epsilon)^j \lambda_1^{i-1-j}$$

$$\overset{(1)}{=} \lambda_2 \epsilon \sum_{i=1}^{n} \lambda_1^{i-1} \frac{(1 + \frac{\epsilon}{\lambda_1})^i - 1}{\frac{\epsilon}{\lambda_1}}$$

$$\overset{(2)}{=} \lambda_2 \left(\frac{(\lambda_1 + \epsilon)^{n+1} - (\lambda_1 + \epsilon)}{(\lambda_1 + \epsilon) - 1} - \frac{\lambda_1^{n+1} - \lambda_1}{\lambda_1 - 1} \right). \blacksquare$$

Let $A_{i,j}$ denotes the (i,j)th element of matrix A and $B_{i',j'}$ denotes the (i',j')th element of matrix B, where $i \in [N_x], j' \in [N_y]$, and $j, i' \in [N_z]$. We now set the maximum value of all $|A_{i,j}|$ (and $|B_{i',j'}|$) as an upper bound to the absolute value of each entry in the A_k and B_k submatrices. We bound each y_k by their largest absolute value, $\max_k |y_k|$. These settings let us apply Lem. 1 to the decoding polynomial, $\tilde{S}_A(x)\tilde{S}_B(x)$. Using the same notation as Lem. 1, we use λ_1 to denote $\max_k |y_k|$ and λ_2 to denote $(\max_{i,j} |A_{i,j}|)(\max_{i',j'} |B_{i',j'}|)$. Since the m fastest workers evaluate the $\tilde{S}_A(x)\tilde{S}_B(x)$ polynomial at $x \in \{z_{k,j_{k,i}}\}_{k\in[K], i\in[m_k]}$, we bound $|\tilde{C}_m - C_m|$ from above as follows. We first use the triangle inequality to upper bound $|\tilde{C}_m - C_m|$ as

$$\sum_{k=1}^{K} |\alpha_k| \frac{\sum_{i=1}^{m_k} |\tilde{S}_A(z_{k,j_{k,i}})\tilde{S}_B(z_{k,j_{k,i}}) - \tilde{S}_A(y_k)\tilde{S}_B(y_k)|}{m_k} \mathbb{1}_{m_k>0}. \tag{15}$$

Note that in above inequality, we use the definitions $\tilde{C}_m = \sum_{k=1}^{K} \alpha_k \frac{\sum_{i=1}^{m_k} \tilde{S}_A(z_{k,j_{k,i}})\tilde{S}_B(z_{k,j_{k,i}})}{m_k}$ and $C_m = \sum_{k=1}^{K} \alpha_k \frac{\sum_{i=1}^{m_k} \tilde{S}_A(y_k)\tilde{S}_B(y_k)}{m_k}$ from Sec. IV. Using Lem. 1, we further upper bound (15) as

$$\sum_{k=1}^{K} \frac{|\alpha_k|}{m_k} \lambda_2 \left(\frac{(\lambda_1 + \epsilon)^{2K-2} - (\lambda_1 + \epsilon)}{(\lambda_1 + \epsilon) - 1} - \frac{\lambda_1^{2K-2} - \lambda_1}{\lambda_1 - 1} \right) \mathbb{1}_{m_k>0}$$

$$\leq \lambda_2 \left(\frac{(\lambda_1 + \epsilon)^{2K-2} - (\lambda_1 + \epsilon)}{(\lambda_1 + \epsilon) - 1} - \frac{\lambda_1^{2K-2} - \lambda_1}{\lambda_1 - 1} \right) \sum_{k=1}^{K} |\alpha_k|.$$

As ϵ goes to zero, the right-hand-side of the above inequality converges to 0, thus $\lim_{\epsilon \to 0} \tilde{C}_m = C_m$. $\blacksquare$

E. Recovery threshold of group-wise SAC

In this section, we first prove that when multi-group SAC uses only $D = 2$ groups, then its recovery threshold is equal to that of two-group SAC. We then prove that if $D > 2$, $R_{\text{G-SAC}} > 2K - 1$. Substituting $D = 2$ in $R_{\text{G-SAC}} = (\sum_{d=1}^{D} 2^{D-d} K_d) + K_D - 1$, we get to $R_{\text{G-SAC}} = (2K_1 + K_2) + K_2 - 1 = 2K - 1$ which equals to that of two-group SAC. When $D > 2$,

$$R_{\text{G-SAC}} = (\sum_{d=1}^{D} 2^{D-d} K_d) + K_D - 1$$

$$\geq \left(K_D + \sum_{d=1}^{D-1} 2K_d \right) + K_D - 1$$

$$= 2 \left(\sum_{d=1}^{D} K_d \right) - 1 = 2K - 1. \blacksquare$$